NASA TECHNICAL NOTE

NASA TN D-7878

NASA TN D-7878

EFFECT OF DESIGN FEATURES ON PERFORMANCE OF A DOUBLE-ANNULAR RAM-INDUCTION COMBUSTOR

Donald F. Schultz

Lewis Research Center
Cleveland, Ohio 44135

NATIONAL AERONAUTICS AND SPACE ADMINISTRATION • WASHINGTON, D. C. • AUGUST 1975

1. Report No.	2. Government Accession No.	3. Recipient's Catalog No.
NASA TN D-7878		

4. Title and Subtitle	5. Report Date
EFFECT OF DESIGN FEATURES ON PERFORMANCE OF A DOUBLE-ANNULAR RAM-INDUCTION COMBUSTOR	August 1975
	6. Performing Organization Code

7. Author(s)	8. Performing Organization Report No.
Donald F. Schultz	E-8210
	10. Work Unit No.
9. Performing Organization Name and Address	505-04
Lewis Research Center National Aeronautics and Space Administration Cleveland, Ohio 44135	11. Contract or Grant No.
	13. Type of Report and Period Covered
12. Sponsoring Agency Name and Address	Technical Note
National Aeronautics and Space Administration Washington, D.C. 20546	14. Sponsoring Agency Code

15. Supplementary Notes

16. Abstract

An extensive test program was undertaken to determine the effect of many design features such as the size and number of air scoops, and the type of diffuser airflow distrtibution to use to optimize performance of a double-annular ram-induction combustor of 94-cm outer diameter. Six combustor configurations were tested. It was found that a snouted double-annular combustor built with 256 ram-induction air scoops with a combustor open area giving a total pressure loss of 5.0 percent at a diffuser inlet Mach number of 0.25 gave the best overall performance of the configurations tested.

17. Key Words (Suggested by Author(s))	18. Distribution Statement
Jet engine; Combustors (double annular); Combustion efficiency; Air pollution; Exhaust gases	Unclassified - unlimited STAR category 07 (rev.)

19. Security Classif. (of this report)	20. Security Classif. (of this page)	21. No. of Pages	22. Price*
Unclassified	Unclassified	52	$4.25

* For sale by the National Technical Information Service, Springfield, Virginia 22161

CONTENTS

EFFECT OF DESIGN FEATURES ON PERFORMANCE OF A DOUBLE-ANNULAR RAM-INDUCTION COMBUSTOR

by Donald F. Schultz

Lewis Research Center

SUMMARY

An extensive test program was undertaken to determine the effect of many design features on the performance of a double-annular ram-induction combustor. Double-annular combustors are unique in that they can be built shorter than an annular combustor of comparable heat release and have the advantage of radial fuel staging. Combustors of 512 and 256 air scoops (for a full annulus) were evaluated using two different combustor open areas so both scoop number and combustor total pressure loss effects were evaluated. Also two diffuser air distribution techniques, snouted combustors and airflow distributing plates, were evaluated to determine an efficient method of distributing the diffuser inlet airflow to the combustor passages.

It was found that a snouted double-annular combustor built with 256 ram-induction air scoops with a combustor open area giving a total pressure loss of 5.0 percent at a diffuser inlet Mach number of 0.25 gave the best overall performance of the combustor-diffuser air distribution configurations tested.

INTRODUCTION

This report covers a five-year test program which was undertaken to determine the effects of the major design features of diffuser airflow distribution, combustor open area and number of air scoops on the performance of a double-annular ram-induction combustor. This program was initiated following sector testing reported in references 1 and 2 and full annular tests reported in references 2 and 3, which

demonstrated the potential of double-annular combustors. The sector testing was performed by Pratt & Whitney Aircraft in Florida while the full annular testing was done in the Engine Components Research Laboratory, a connected duct facility, at the Lewis Research Center.

Double-annular combustors have two basic features of merit - short length and the capability of radial fuel staging. The ram-induction concept, which uses air scoops with turning vanes rather than simple punched holes to supply most of the primary and secondary combustion air, further minimizes combustor length. Still additional length reduction can be obtained by using shorter length diffusers, which diffuse the air to higher Mach numbers, than is common with conventional combustors.

References 4 to 11 represent work on specific areas of double-annular design or performance which was reported during the testing period of this program. Reference 4 was an air swirler geometry study which compared radial inflow and axial flow air swirlers. That report showed radial inflow air swirlers to be superior to axial flow air swirlers. The design of the ram-induction air scoops was extensively studied in reference 5. The scoop variations of reference 5 included scoop discharges inclined 45^{o} upstream, circumferentially directed secondary scoops, (scoops inclined to the combustor radius thus producing circumferential flow as well as radial flow compared to only radial flow with conventional scoops), and variations in liner open area distribution between primary and secondary scoops and the distribution of air between the outer, inner, and center liners. The original scoop design, which introduced the air radially was found to provide the best all around performance in reference 5.

References 4 and 6 to 10 give information on combustor idle emissions and relative altitude relight ability. Some combustor variable geometry techniques such as a translating outer exit transition liner, and variable snout inlet were studied in references 7 and 8. This work which was directed at reducing exhaust emissions at ground idle and improving altitude relight capability was quite successful. Also a program was conducted to determine the effects of radial and circumferential inlet velocity profile distortions. The double-annular combustor was found to be unaffected by radial inlet air velocity distortions, but was sensitive to circumferential distortions, as pattern factor was found to increase substantially. Further information on inlet air distortions is given in reference 11.

The purpose of the present report is to compare the full annular combustor configurations reported in references 1 to 11 with other unreported configurations, to evaluate the various combustor design features. The combustor comparisons are based on total pressure loss, combustion efficiency, exit temperature profiles, exit temperature parameters, altitude relight capability, and levels of pollutant exhaust emissions.

A variety of test conditions were used in testing at Lewis for this program. Two test points simulated sea-level takeoff conditions (except for pressure) of approximately 12-to-1 and a 23-to-1 pressure ratio turbofan engines. Also two supersonic cruise points were used. They were comparable to a Mach 2.7 flight speed which was representative of the U.S. SST airplane proposed for the late 1960's and a Mach 3.0 flight cruise point to evaluate the durability, the rate at which the combustor deteriorates with time, and emissions caused by a higher inlet-air temperature.

APPARATUS

Combustor Design

The double-annular concept. - The combustor used in this investigation is referred to as a double-annular ram-induction combustor. Constructing the combustion zone as a double annulus permits the reduction of overall combustor length while maintaining an adequate ratio of length to annulus height in each combustion zone. Figure 1 shows a typical double-annular combustor. This double-annular feature allows a considerable reduction in length to be made over a single annulus with the same overall height. Individual control of the inner and outer annulus fuel systems of the double-annular combustion zone provides a useful method for adjusting the outlet radial temperature profile. This individual fuel control also permits the use of radial fuel staging for low power settings such as ground idle and altitude relight.

The ram-induction concept. - The ram-induction combustor differs from the more conventional combustors in that the compressor discharge air is allowed to penetrate into the combustion and mixing zones without diffusing to as high a static pressure as a conventional static pressure-fed combustor. The kinetic energy of the inlet air is thereby used to promote rapid mixing of air and fuel in the primary zone and diluent air and burned gases in the mixing zone. The airflow is efficiently turned into

the combustor by two rows of vaned turning scoops that penetrate into the combustion zones.

The ram-induction combustor has the following advantages over conventional static pressure-fed combustors:

(1) A shorter length combustor is obtained because more controlled mixing can be established in the combustion zone. This mixing is achieved by better control of the airflow injection angle with the vaned turning scoops.

(2) Diffuser length can be shortened since diffusion to very low combustor air velocities is no longer needed or desired. The overall diffuser-combustor length can, therefore, be reduced. The small area ratio diffuser in the shorter length could have less pressure loss since it is not as prone to flow separation as diffusers of larger area ratios. However, this advantage can be offset by the increased turning losses associated with splitting the relatively high velocity flow evenly between the combustor airflow passages and the combustor itself.

(3) The high velocity flow over the exterior surfaces of the combustor provides substantial convective cooling of these walls. This convective cooling reduces the film cooling air requirements. Thus more air is available for mixing and temperature profile control.

A more detailed discussion of the ram-induction concept is provided in reference 12.

Combustor design details. - Table I summarizes the configuration of each model. Six double-annular ram-induction diffuser-combustor combinations were compared in this investigation.

The double-annular combustors have three primary airflow passages fed by the diffuser. They are the inner, center, and outer shrouds as shown in figure 2. Forty to sixty percent of the airflow depending on the model is ducted to the outer and inner liners of the combustors. The remaining air enters the headplate, center shroud, and exit transition liners. The high velocity airflow which is maintained from the diffuser inlet through this ducting is turned into the combustor burning zones by means of the scoops. The first row of scoops supplies air to the primary zone, while the second row supplies diluent air to the secondary zone (see fig. 1).

Three types of diffuser arrangements were evaluated. Three of the combustor models used diffuser airflow splitter plates, two used snouts and one used an open diffuser. Two of the combustors had 512 airflow scoops and four had 256 scoops. Two combustors had open hole areas of about 1070 square centimeters and four had

open hole areas of about 1430 square centimeters.

Basic dimensions of the combustors are shown in figure 2. The diameters are essentially those of the combustor for the Pratt & Whitney Aircraft experimental supersonic transport engine (JTF 17 (ref. 13)). However, the diffuser-combustor overall length of the double-annular combustor is about 30 percent shorter than that used in the JTF 17 engine.

Photographs of the combustor types are shown in figures 3 to 5. Comparing figures 3 and 4 shows the complexity of the 512 scoop combustors compared to the simpler 256 scoop types.

Figure 5 is a sideview showing the snout and airflow splitter plate types of diffuser airflow distributors.

Combustor design specifications. - The major items in the combustor design are tabulated in table II. The circumferential locations of combustor components such as scoops, fuel nozzles, and diffuser struts are shown in figure 6. The flow areas as distributed among the many openings (scoops, film cooling, swirlers, etc.) are given on the combustor sketch of figure 7 and in table III as well as scoop length and width dimensions for the different models tested.

Fuel nozzles. - Simplex fuel nozzles with axial or radial inflow air swirlers were used for the investigation. Table IV shows the fuel nozzle characteristics at the various test conditions. Figure 8 shows the axial and radial inflow air swirlers used in this study.

Test Facility

The full-scale double-annular ram-induction combustor investigation was conducted in a closed-duct test facility of the Engine Components Research Laboratory at Lewis. A schematic of this facility is shown in figure 9. Airflows for combustion ranged from 2.3 to 136 kilograms per second at pressures ranging from 1.7 to 113.8 newtons per square centimeter. Air temperatures could be controlled over a range of 265 to 922 K without vitiation before entering the combustor under test.

For combustor inlet-air temperatures of 589 K or less, an indirect-fired heat exchanger was used. For higher inlet temperatures (to 922 K), a second stage of indirect heating was used. Heat for the second stage was provided by a natural-gas-fueled J-57 jet engine with afterburner.

Figure 10 shows the combustor test section and the connected inlet and outlet ducting. About $4\frac{1}{2}$ pipe diameters of constant area duct was ahead of the test section, which included the diffuser inlet and diffuser as part of the housing. The combustor housing measured 1.02 meters at the maximum diameter and was 0.96 meter long including the inlet section. Following the combustor housing was the outlet instrumentation section. Downstream of this section, the combustor exhaust gases were cooled by a water-injection spray system. The exposed surfaces downstream of the combustor were cooled by two methods: (1) circulating water in passages adjacent to the hot surfaces, and (2) water sprays impinging directly on the exposed surfaces.

Airflow rates and combustor pressures were regulated by remotely controlled valves upstream and downstream of the test section. Flow straighteners were used to evenly distribute the airflow entering the combustor (see fig. 10).

Instrumentation

Measurement methods. - Measurements to determine combustor operation and performance were recorded by the Lewis Central Automatic Data Processing System (ref. 14). Control room readout instrumentation (indicating and recording) was used to set and monitor the test conditions and the operation of the combustor. Pressures were measured and recorded by the central Digital Automatic Multiple Pressure Recorder (DAMPR) and by strain-gage pressure transducers (ref. 15). Iron-constantan thermocouples were used to measure temperatures between 240 to 675 K; Chromel-Alumel thermocouples measured temperatures between 240 and 1560 K. High temperatures (to 1920 K) were measured with platinum 13 rhodium-platinum thermocouples. The indicated readings of all thermocouples were taken as true values of the total temperatures. The platinum 13 rhodium-platinum thermocouples (Type R) were of the high-recovery aspirating type (ref. 16, type 6).

Airflow rates were measured by square-edged orifices installed according to ASME specifications. Fuel flow rates were measured by turbine flowmeters using frequency-to-voltage converters for readout and recording.

Instrumentation stations. - The locations of the combustor instrumentation stations are shown in figure 2. Inlet air temperature was measured by eight Chromel-Alumel thermocouples that were equally spaced around the inlet at station 3.

The pressure rakes measured the total pressure profile at centers of equal areas across the inlet annulus. Static pressure at the inlet was measured by sixteen wall static pressure taps with eight on the outer and eight on the inner walls of the annulus at station 3.

Combustor shroud instrumentation consisted of six rakes to measure airflow distribution between the outer, inner, and center flow passages at station 3.5 as defined in figure 2. Each rake consisted of three total pressure tubes (except the snout rakes which contained four) and a static pressure tube. These rakes were located at the entrance to each flow passage and the tubes were at centers of equal area. In the case of the snouted combustors the center flow passage was measured at the snout inlet rather than station 3.5.

Combustor outlet total temperature and pressure at instrumentation station 4 were measured at 3^{o} increments around the exit circumference. At each 3^{o} increment, five temperature and five pressure points were measured across the annulus. Three of these probes, each on an arm 120^{o} apart, rotated 120^{o} providing full coverage of the circumference. Water-cooled shields protected these probes when they were not in use at three fixed points in the exhaust stream. At these points, temperature and pressure were not measured. The portion of the probes exposed to the hot exhaust gases were made of platinum-rhodium alloy. Also located at station 4 were eight wall static pressure taps.

Two methods were used to obtain exhaust gas samples. Eight randomly spaced five point fixed sample probes were used in the early testing while three five point rotating sample probes were used in the later tests. Figure 11 shows examples of the gas sample probes used. In all cases, steam traced lines were used to maintain gas sample temperatures near 435 K.

PROCEDURE

Test Conditions

For this investigation four test conditions were selected. Two conditions simulate takeoff of low and high pressure ratio fan engines except for proper pressure which could not be obtained in this facility. Two conditions simulate cruise of a

supersonic turbofan engine. Table IV outlines the test conditions used. A design exit temperature of 1478 K was used for all conditions. ASTM-Jet A fuel was used throughout this investigation. JP-4 was used in some altitude relight tests of reference 6.

Calculations

Combustion efficiency by thermocouple measurement. - Efficiency was determined by dividing the measured temperature rise across the combustor by the theoretical temperature rise. The theoretical rise is calculated from the fuel-air ratio, fuel properties, inlet air temperature, and pressure, as well as the amount of water vapor present in the inlet airflow. The exit temperatures were measured with five-point traversing aspirated thermocouple probes and were mass weighted for the efficiency calculation. The indicated readings of all thermocouples were taken as true values of the total temperatures. The mass-weighting procedure is given in reference 13. In each mass-weighted average, 585 individual exit temperatures were used.

Combustion efficiency by gas analysis. - Efficiency by gas analysis was determined by measuring the amount of carbon dioxide, carbon monoxide, and unburned hydrocarbons in the exhaust gas. Multiple gas samples were obtained as described in the section Instrumentation. An analysis of 39 samples was made during each data point. The derived combustion efficiency calculated from gas analysis was validated by determining the combustor fuel-air ratio from the exhaust analysis. This fuel-air ratio was then divided by the metered fuel-air ratio to obtain fuel-air-ratio ratio (FARR) to compare their agreement. A value of 1.0 indicates that fuel-air ratios computed by carbon balance from gas sampling are in complete agreement with fuel-air ratio based on metered air and fuel flows.

An additional check on gas sample validity was made on selected data points. For this check the remaining oxygen in the exhaust was measured and the fuel-air ratio was calculated based on oxygen depletion. The fuel-air ratio by oxygen analysis was then divided by the metered fuel-air ratio to compare their agreement. This ratio is called FARRO and is listed along with FARR values in the data table (table V). FARR and FARRO values of 1.0 ± 0.05 for late data or ± 0.15 for early

data were considered acceptable values.

Reference velocity and diffuser inlet Mach number. - Reference velocity V_{ref} for the combustor was computed from the total airflow reference area (the maximum cross-sectional area between the inner and outer shroud) (see table II), and the diffuser inlet total pressure and temperature. Diffuser inlet Mach number was calculated from the total airflow, the total temperature and the static pressure measured at the diffuser inlet, and the inlet annulus area.

Total pressure loss. - The total pressure loss $\Delta P/P$ was calculated by mass averaging total pressures measured upstream of the diffuser P_{t3} inlet and at the combustor exit. The total pressure loss, therefore, includes the diffuser loss.

Exit temperature profile parameters. - Four parameters of interest in evaluating the quality of exit temperature profile are considered. They are pattern factor, local factor, stator factor, and rotor factor. Pattern factor and local factor are used for preliminary screening, while the parameter δ_{stat} is a measure of the quality of the exit temperature profile on the turbine stator, and δ_{rot} is a measure of the quality of the exit temperature profile on the turbine rotor. Figure 12 is a graphical explanation of these parameters. The exit temperature pattern factor is defined as

$$\overline{\delta} = \frac{T_{t4(max)} - T_{t4}}{T_{t4} - T_{t3}}$$

where T_{t4} and T_{t3} are averages of temperatures measured at the exit and inlet, and where $T_{t4(max)} - T_{t4}$ is the maximum temperature occurring anywhere in the combustor exit plane minus the average exit temperature. The exit temperature local factor δ_{loc} is defined as

$$\delta_{loc} = \frac{T_{t4(loc)} - T_{t4}}{T_{t4} - T_{t3}}$$

where $T_{t4(loc)} - T_{t4}$ is the local temperature occurring anywhere in the combustor exit plane minus the average exit temperature. Local factor equals pattern factor at the point of greatest positive temperature difference. These parameters are useful for preliminary screening, but do not take into account the desired radial

temperature profile for which the combustor was designed. The desired average radial distribution of temperature at the combustor exit plane is determined by the stress and cooling characteristics of the turbine. For purposes of evaluating the double-annular combustor, an exit radial temperature profile was selected for conditions that are typical of advanced engines.

The two other parameters take the design profile into account. These parameters are

$$\delta_{stat} = \frac{\left[T_{t4j(loc)} - T_{t4j(des)}\right]_{max}}{T_{t4} - T_{t3}}$$

$$\delta_{rot} = \frac{\left[T_{t4j} - T_{t4j(des)}\right]_{max}}{T_{t4} - T_{t3}}$$

where $\left[T_{t4j\,(loc)} - T_{t4j\,(des)}\right]_{max}$ for δ_{stat} is the maximum positive temperature difference between the highest local temperature at any given radius and the design temperature for that same radius (the subscript j refers to any radial location in the radial temperature profile) and where $\left[T_{t4j} - T_{t4j\,(des)}\right]_{max}$ for δ_{rot} is the maximum temperature difference between the average temperature at any given radius around the circumference and the design temperature for that same radius (see fig. 12). The term used in the denominator in all four parameters is the average temperature rise across the combustor ΔT.

Shroud flows. - For the three shroud flows (inner, center, and outer), an airflow was calculated for each total pressure tube all of which were located at centers of equal areas. The individual airflows for each rake were summed. The two rakes in each annular passage were then averaged. The total shroud flow was determined by summing the average flow entering each passage. This flow was used to determine the percentage split between the three annular passages.

Units. - The customary U.S. system of units was used for primary measurements and calculations. Conversion to SI units (Systeme International d'Unités) is done for reporting purposes only. In making the conversion, consideration is given to implied accuracy and may result in rounding off the values expressed in SI units.

RESULTS AND DISCUSSION

Table V is a list of typical test results for the takeoff and cruise operating conditions used in this investigation. ASTM Jet-A fuel was used for all tests. The design average exit temperature of 1478 K was not obtained with all models tested due to excessive local temperature peaks which could damage the exit temperature instrumentation. Radial fuel staging was used in some cases to improve the exit temperature profile.

Airflow Distribution Between Combustor Passages

Figure 13 shows the measured air flow distribution between the combustor shrouds and the percentage of inlet airflow measured by the shroud pressure rakes. In the case of the two snouted combustors, models 6 and 7, the center shroud flow pressure rake was mounted at the snout inlet and contained four total pressure tubes and a static rather than three total pressure tubes and a static when mounted at the inlet to the center shroud. The extra total pressure tube was added due to the greater annulus height. Figure 13 indicates that between 40 and 60 percent of the shroud air went down the center passage. Models 1, 3, and 6 flowed about equal percentages of their remaining air down their outer and inner passages. The remaining three models flowed more of the remaining air to the inner shroud passage than to the outer shroud passage.

Overall performance (when considering total pressure loss exit temperature parameters and durability) indicates that a snouted combustor is best and should distribute about 60 percent of its airflow to the snout and 20 percent to each the outer and inner shroud passages such as in model 6, a snouted combustor with 256 air scoops and small open area. A combustor using splitter plates performed second best. The best combustor design using splitter plates distributed 48 percent of its air to the center shroud and 26 percent to each of the outer and inner shrouds.

Total Pressure Loss

Figure 14 compares combustor total pressure loss which includes the diffuser loss for the models tested at a takeoff and a cruise condition. Dashed curves are provided to indicate calculated pressure losses while the solid curves represent measured pressure losses. Model 7 (a snouted combustor with 256 scoops and larger open area) had the lowest takeoff pressure loss which was only 4.1 percent. Model 6 (a snouted combustor with 256 scoops and small open area) was second best at 5.1 percent. Model 10A (a combustor with open diffuser, 256 scoops, and larger open area), which was model 10 with the diffuser flow splitters removed, had a lower pressure loss than model 10. However, figure 13 shows the airflow distribution was very poor with model 10A when compared to any other model. On model 10A nearly as much air flowed in the inner shroud passage as in the center. This led to liner durability problems.

Model 6 had the lowest pressure loss of any of the combustors tested at the Mach 3.0 cruise condition, 7.25 percent. Figure 15 shows model 6's total pressure loss as a function of diffuser inlet Mach number over the range of conditions tested. Snouted combustors provided lower pressure losses than did comparable splitter plate flow distributing combustors.

Exit Temperature Distribution Parameters

Figure 16 compares the exit temperature profile parameters of pattern factor, stator factor, and rotor factor for the combustors tested at up to four simulated engine conditions. This comparison was made at 1478 K exit average temperature except for model 3 which was only tested to 1381 K due to the high local temperatures encountered. This figure shows that pattern and stator factors for the better configurations remained below 0.2 for these test conditions, while the rotor factor usually remained below 0.03. These values are consistent with good design practice. Model 6 (a snouted combustor with 256 scoops and small open area) performed best of all the combustors tested having exit temperature parameters of pattern factor and stator factor lower than any other combustor at all conditions except Mach 3.0 cruise. At Mach 3.0 cruise the pattern factor of model 10 (a 256 scoop combustor

with larger open area and splitter plates) was 0.143 versus 0.169 for model 6. However, at this same condition model 6's stator factor was only 0.168 versus 0.201 for model 10. Comparing rotor factor at takeoff condition 5 (table IV), model 6 outperformed all other models except model 1B (a 512 scoop combustor with small open area and splitter plates) at Mach 3.0 cruise condition (and model 7, a snouted combustor with 256 scoops and large open area).

Radial fuel staging. - Radial fuel staging is a process of adjusting the exit temperature profile by varying the ratio of fuel flow to each annulus. Figure 17 shows the effect of radial fuel staging on pattern factor, stator factor, and rotor factor for the model 6 combustor at a simulated takeoff condition with 590 K inlet temperature air. A 30 percent reduction in pattern and stator factors was achieved by flowing 20 percent more fuel to the inner annulus than to the outer annulus. Though less significant, a reduction in rotor factor from 0.032 down to 0.025 was obtained with the same radial fuel staging that gave the 30 percent reduction in pattern and stator factors. Radial fuel staging was not employed on all models, but when used the radial fuel split giving the lowest exhaust temperature parameters was used in this presentation. The relative merits of the configurations are not affected by the comparisons made at different fuel splits. A comparison of all models with the same fuel flow in each annulus showed that snouted combustors had the lowest exit temperature parameters.

Exit temperature analysis technique. - A technique was developed at Lewis Research Center to permit research engineers to evaluate combustor exit temperature profiles very quickly. A unique computer program was prepared which converts exit temperatures into local factor. Figure 18 employs this technique. With this format, local factor increases chronologically with the alphabet for positive values and chronologically with numbers for negative values. Thus, as the key shows in figure 18, a "B" would indicate a hot spot that would result in a local factor between 0.1 and 0.2, and conversely a "2" would correspond to a cold spot "local factor" between -0.1 and -0.2. Pattern factor as normally reported would be the largest positive value of local factor.

Figures 18(a) to (d) show the combustor exit temperature patterns machine coded in terms of local factor for model 6 combustor at the four test conditions. Shading is used to show the hottest, highest local factor, areas.

Figure 18(e) is a typical exit local factor distribution for model 3, which was

the poorest performing model from an exit temperature distribution standpoint.

Radial temperature profile. - Figures 19(a) and (b) compare the average radial and peak radial temperature profiles to the design radial temperature profile at the takeoff and Mach 3.0 cruise operating conditions for the combustor models tested. These figures show the temperature profile entering the engine stator and turbine. As the stator blades are stationary, they must be built to withstand the peak temperature profile while the turbine need only be built to withstand the average radial temperature profile. Design practice favors a slightly tip peaked temperature profile similar to the design radial temperature profile, to reduce peak temperatures at the turbine peak stress point, the hub. Models 3 and 7 are not shown in figure 19(b) since they were not tested at the Mach 3.0 cruise condition. Figure 19 shows that the model 6 combustor had the lowest average and peak temperature deviations of any of the combustors at takeoff and was nearly comparable to model 10 at the Mach 3.0 cruise condition. Even at the Mach 3.0 cruise condition, model 6's profile may provide a less severe environment for the stator vanes and turbine than model 10 since model 6's hub temperatures are lower than model 10's.

Combustion Efficiency

Combustion efficiency as computed by exhaust gas analysis was 99.6 percent or higher for both the takeoff and cruise conditions for all the models tested at each condition. Combustion efficiency measured by thermocouples varied from 97.8 to 104.5 percent. Thermocouple combustion efficiency data in table V is included as exhaust gas analysis was unavailable for the early testing in this program.

Altitude Relight

The relative altitude relight capability of four of the combustor models was evaluated using ambient temperature air and fuel at a combustor reference Mach number of 0.05. This is an arbitrary condition used for comparative purposes only. In this test, an altitude relight was defined as ignition with a minimum resulting temperature rise of 80 K the lowest temperature rise that was considered adequate to accelerate an engine of this size.

Figure 20 summarizes the results of these tests. Model 1B (a 512 scoop combustor with small open area and splitter plates) performed best by relighting at 5.5 newtons per square centimeter inlet total pressure and 287 K inlet air temperature. Model 6 (a snouted combustor with 256 scoops and small open area) was a very close second with ignition at 5.5 newtons per square centimeter and 292 K. Other altitude relight information, including use of variable combustor geometry (simulated translating exit transition liner, and flapper valves on the snout inlet), with model 6 is given in reference 8. Relights down to 3.6 newtons per square centimeter inlet pressure with 285 K inlet temperature air and 80 K temperature rise were obtained by simulating variable combustor geometry. A dashed curve is provided in figure 20 to show typical altitude relight performance. This curve is taken from reference 6 (fig. 11(b)) and represents a 100 K temperature rise versus 80 K temperature rise as specified for ignition for the data points in figure 20.

Exhaust Emissions

Because of the high combustion efficiency encountered (in excess of 99.6 percent) with all models, presentation of exhaust emissions of unburned hydrocarbons and carbon monoxide emission indices is limited to the table V as these values were found to be insignificant.

Extensive carbon monoxide and unburned hydrocarbon emissions information at engine ground idle conditions, including the effects of variable combustor geometry used to reduce emissions at idle is given in references 4 and 8 to 10. Radial fuel staging, radial inflow air swirlers, and variable combustor geometry similar to that described in the altitude relight section all reduced exhaust emissions of unburned hydrocarbons and carbon monoxide. Reference 9 also provides parametric emissions information over a range of combustor inlet air temperatures of 585 to 895 K, inlet pressures of 20 to 62 newtons per square centimeter, reference velocities of 24 to 48 meters per second, and exit average temperatures of 1250 to 1478 K with a few points as low as 815 K.

Oxides of nitrogen emissions are shown in figure 21, a bar chart comparing the combustor models tested at simulated takeoff and cruise. This figure shows that diffuser airflow distribution technique has little effect on NO_x emissions. Models 7,

10, and 10A all produced a NO_x emissions index of about 9.5 grams per kilogram fuel at the simulated takeoff condition with 755 K inlet air temperature. Using the extrapolation technique of reference 17, this NO_x emission index increases to 18.0 grams per kilogram fuel at a pressure ratio of 23 to 1, a design compression ratio representative of large turbofan engines. Comparing models 7, 10, and 10A figure 21 also shows that combustor total pressure loss has little or no effect on oxides of nitrogen emissions as the oxides of nitrogen emissions index was 9.5±0.1 gram per kilogram of fuel for all three models at the S_2 takeoff simulated condition while total pressure loss varied from 5.5 percent for model 7 to 7.2 percent for model 10. Model 6 produced somewhat higher NO_x than model 10 at the cruise conditions. Higher combustion temperatures are known to increase oxides of nitrogen emissions. Extrapolating data of model 3 at simulated takeoff from 1381 K exit average temperature to 1475 K exit average temperature using reference 9 increases the oxides of nitrogen emission index from 5.6 to 6.4 making model 3 the highest emitter at that condition. A comparison of models 3 and 10 at the S_1 takeoff condition shows that oxides of nitrogen decrease with increasing scoop size. A similar comparison exists for models 6 and 10 at cruise, where model 10 which has larger scoops also has lower oxides of nitrogen emissions.

Durability

Table VI shows the accumulated burning time for each of the combustor models tested. Included in these times is time accumulated from other double-annular test programs. Models 1, 6, and 10 were operated for over 100 hours each at conditions ranging from idle to Mach 3.0 cruise with only minor liner burning and warpage of scoops an example of which is shown in the circled areas of figure 22. Models 3 and 7 were not tested extensively but exhibited only minor distress, whereas model 10A suffered considerable burning and warpage of short center scoops during its 20.4 hours of testing. Model 10A's durability problems are related to the reduced airflow in the center shroud. Model 10A flows only 40.3 percent of its air in the center liner compared to 43.8 percent for model 10 and 48.9 percent for model 1.

CONCLUDING REMARKS

It appears that a double-annular combustor of the basic size investigated, 94-centimeter external diameter, should be a snouted combustor with 256 ram-induction air scoops, an open area of about 1100 square centimeters, and of similar construction to model 6. The model 6 combustor (a snouted combustor with 256 scoops and a small open area) was found to perform best overall. Its total pressure loss was among the lowest tested being 5.1 percent at simulated takeoff with 590 K inlet air temperature. Model 6's pattern factor was below 0.19, stator factor was below 0.17, and rotor factor was below 0.028 for all conditions tested giving the best overall exit temperature profile performance. Model 6 also exhibited about the best altitude relight performance by relighting with 80 K temperature rise at an inlet condition of 0.05 reference Mach numbers, 5.5 newtons per square centimeter inlet total pressure, and 292 K inlet temperature. NO_x emissions, however, were somewhat higher than for the other models reaching values of 12.4 and 16.8 grams per kilogram fuel respectively at the Mach 2.7 and Mach 3.0 cruise conditions. Model 6's durability appeared to be among the best with minimal deterioration after 105 hours of operation.

Snouted combustors were found to be superior to splitter plate or open diffusers when exit temperature profile, durability, and total pressure loss are considered. Snouted combustors had higher pressure losses than open diffusers, but open diffusers provided very poor airflow distribution compared to very good airflow distributions for snouted combustors. The 256 scoop combustors were found to be as good or better than 512 scoop combustors when considering durability, exit temperature profile, and exhaust emissions of oxides of nitrogen.

Lewis Research Center,
National Aeronautics and Space Administration,
Cleveland, Ohio, March 14, 1975,
505-04.

REFERENCES

1. Kitts, D. L.: Development of a Short-Length Turbojet Combustor. (PNA-FR-2433, Pratt & Whitney Aircraft; NAS3-7905.), NASA CR-54560, 1968.

2. Perkins, Porter J.: Comparison of Test Results from a 90 deg Sector and a Full Annulus Advanced Turbojet Combustor. NASA TM X-52707, 1969.

3. Perkins, Porter J.; Schultz, Donald F.; Wear, Gerrold D.: Full Scale Tests of a Short Length, Double Annular Ram Induction Turbojet Combustor for Supersonic Flight. NASA TN D-6254, 1971.

4. Schultz, Donald F.: Modifications that Improve Performance of a Double Annular Combustor at Simulated Engine Idle Conditions. NASA TM X-3127, 1974.

5. Clements, T. R.: A 90 degree Sector Development of a Short Length Combustor for a Supersonic Cruise Turbofan Engine. (PWA FR-3790, Pratt & Whitney Aircraft; NAS3-11159.), NASA CR-72734, 1970.

6. Schultz, Donald F. and Mularz, Edward J.: Factors Affecting Altitude Relight Performance of a Double-Annular Ram-Induction Combustor. NASA TM X-2630, 1972.

7. Schultz, Donald F.: Variable Combustor Geometry for Improving the Altitude Relight Capability of a Double Annular Combustor. NASA TM X-3163, 1974.

8. Schultz, Donald F.: Ground Idle Performance Improvement of a Double-Annular Combustor by Using Simulated Variable Combustor Geometry. NASA TM X-3176, 1974.

9. Schultz, Donald F.: Exhaust Emissions of a Double Annular Combustor - Parametric Study. NASA TM X-3164, 1974.

10. Clements, T. R.: Effect of Fuel Zoning and Fuel Nozzle Design on Pollution Emissions at Ground Idle Conditions for a Double-Annular Ram-Induction Combustor. (PWA FR-5295, Pratt & Whitney Aircraft; NAS3-11159.), NASA CR-121094, 1973.

11. Schultz, Donald F.; Perkins, Porter J.: Effects of Radial and Circumferential Inlet Velocity Profile Distortions on Performance of a Short-Length Double-Annular Ram-Induction Combustor. NASA TN D-6706, 1972.

12. Chamberlain, John: The Ram Induction Combustor Concept. Presented at 3rd, AIAA Propulsion Joint Specialist Conference, Washington, D.C., July 7, 1967.

13. Rusnak, J. P.; and Shadowen, J. H.: Development of an Advanced Annular Combustor. (PWA-FR-2832, Pratt & Whitney Aircraft; NAS3-9403.), NASA CR-72453, 1969.

14. Staff of the Lewis Laboratory: Central Automatic Data Processing System. NACA TN 4212, 1958.

15. Mealey, Charles; and Kee, Leslie: A Computer-Controlled Central Digital Data Acquisition System. NASA TN D-3904, 1967.

16. Glawe, George E.; Simmons, Frederick S.; and Stickney, Truman M.: Radiation and Recovery Corrections and Time Constants of Several Chromel-Alumel Thermocouple Probes in High-Temperature, High-Velocity Gas Streams. NACA TN 3766, 1956.

17. Shaw H.: The Effects of Water, Pressure, and Equivalence Ratio on Nitric Oxide Production in Gas Turbines. ASME Paper 73-WA/GT-1, Dec. 1973.

TABLE I. - CONFIGURATION SUMMARY

OF COMBUSTOR MODELS TESTED

Model	Diffuser aid	Number of air scoops	Total open area, cm^2
1	Splitter plate	512	1040
3	Splitter plate	512	1455
6	Snout	256	1098
7	Snout	256	1431
10	Splitter plate	256	1431
10A	None	256	1431

TABLE II. - DOUBLE-ANNULAR RAM-INDUCTION

COMBUSTOR DIMENSIONS AND SPECIFICATIONS

Length, cm	
Compressor exit to turbine inlet	51.1
Fuel nozzle face to turbine inlet	30.5
Diameter, cm	
Inlet outside	80.77
Inlet inside	71.1
Outlet outside	89.9
Outlet inside	69.9
Shroud diameter, cm	
Outside	94.2
Inside	57.2
Reference area (between shrouds), cm^2	4270
Diffuser inlet area, cm^2	1177
Exit area, cm^2	2503
Number of fuel nozzles and swirlers	64
Number of diffuser struts	16
Rows, primary zone	1
Rows, secondary zone	1
Ratio length to annulus height	
Outer annulus	4.8
Inner annulus	3.9

TABLE III. - TOTAL SCOOP AREAS AND SIZES FOR DOUBLE-ANNULAR COMBUSTOR MODELS TESTED

[Model 10 A scoop dimensions same as model 10 scoop dimensions.]

Type of scoop and its dimensions (see fig. 7)	Model				
	1	3	6	7	10
A. Outer liner primary					
Discharge area, cm^2	80.516	125.95	87.21	122.73	122.73
Length, cm	1.163	1.422	1.674	1.979	1.979
Width, cm	1.163	1.384	1.628	3.835	3.835
B. Outer liner secondary					
Discharge area, cm^2	142.864	223.04	154.79	218.64	218.64
Length, cm	1.560	1.890	2.225	2.637	2.637
Width, cm	1.560	1.844	2.174	2.591	2.591
C. Outer center shroud primary					
Discharge area, cm^2	80.516	125.95	87.05	122.85	122.85
Length, cm	1.163	1.422	1.671	1.981	1.981
Width, cm	1.163	1.384	1.628	1.938	1.938
D. Outer center shroud secondary					
Discharge area, cm^2	71.432	111.89	76.35	109.03	109.03
Length, cm	1.560	1.890	2.200	1.295	1.295
Width, cm	.803	.925	1.085	3.407	3.407
E. Inner center shroud primary					
Discharge area, cm^2	80.516	125.95	87.05	122.85	122.85
Length, cm	1.163	1.422	1.671	1.981	1.981
Width, cm	1.163	1.384	1.628	1.938	1.938
F. Inner center shroud secondary					
Discharge area, cm^2	71.432	111.89	76.35	109.03	109.03
Length, cm	1.560	1.89	2.200	1.295	1.295
Width, cm	.803	.925	1.085	3.407	3.407
G. Inner liner primary					
Discharge area, cm^2	80.929	123.71	87.61	122.35	122.35
Length, cm	1.222	1.623	1.755	2.07	2.07
Width, cm	1.112	1.191	1.560	1.847	1.847
H. Inner liner secondary					
Discharge area, cm^2	146.58	221.89	156.59	219.25	219.25
Length, cm	1.963	2.532	2.809	3.31	3.31
Width, cm	1.245	1.369	1.742	2.07	2.07
I. Outer annulus swirlers					
Type	Radial	Axial	Axial	Axial	Axial
Area, cm^2	72.76	72.76	69.92	69.92	69.92
J. Inner annulus swirlers					
Type	Radial	Axial	Axial	Axial	Axial
Area, cm	72.76	72.76	69.92	69.92	69.92
Flow spreader or snout inlet areas					
Outer passage, cm^2	348	348	476	476	348
Center passage, cm^2	785	785	940	940	785
Inner passage, cm^2	339	339	503	503	339
Number of scoops	512	512	256	256	256

TABLE IV. - TEST CONDITIONS

[Combustor average exit temperature, ~1478 K.]

Test condition	Inlet air conditions				Reference velocity, m/sec	Fuel-air ratio	Fuel-nozzle differential pressure, N/cm^2
	Total pressure, N/cm^2 abs	Total temperature, K	Airflow, kg/sec	Diffuser inlet Mach number			
S_1, simulated takeoff	62	590	50	0.249	30.5	0.0253	230
S_2, simulated takeoff	62	755	50	.287	40.7	.0212	150
C_1, Mach 2.7 cruise	41	840	33	.296	42.7	.0187	64
C_2, Mach 3.0 cruise	62	895	49	.312	45.7	.0171	100

TABLE V. -

Run number	Test condition	Inlet-air conditions				Combustor operating conditions					
		Total pressure, N/cm^2	Total temperature, K	Airflow, kg/sec	Diffuser inlet Mach number	Reference velocity, V_{ref}, m/sec	Fuel air ratio	Average outlet temperature, K	Fuel nozzle differential pressure, N/cm^2	FIDOD, F_{ID}/F_{OD}	Pattern factor, $\overline{\delta}$
Model 1B											
24	S_1	62.1	596	49.4	0.246	31.8	0.0260	1510	237	0.997	0.359
30	S_2	62.0	776	49.4	.287	41.4	.0209	1493	150	.992	.305
37	C_1	41.6	844	32.9	.299	44.6	.0187	1478	55	1.000	.217
46	C_2	62.3	898	49.2	.311	47.5	.0173	1481	103	1.000	.222
Model 3											
786	S_1	62.0	591	49.9	0.247	31.9	0.0221	1389	175	0.970	0.588
799	S_1	61.9	593	50.4	.252	32.5	.0219	1381	170	.949	.431
Model 6											
143	S_1	62.1	597	50.2	0.250	33.3	0.0254	1471	291	1.200	0.1687
148	S_2	61.8	758	50.3	.290	41.3	.0209	1464	183	1.100	.154
153	C_1	41.2	842	32.8	.301	44.8	.0187	1462	56.1	1.005	.145
119	S_1	62.2	593	49.7	.247	31.7	.0257	1479	284	1.156	.188
515	C_1	41.4	841	33.1	.302	45.2	.0186	1462	56.8	.991	.340
503	C_2	62.0	894	49.4	.313	47.8	.0172	1464	106.9	1.006	.187
Model 7											
1327	S_1	61.7	591	49.9	0.249	32.0	0.0258	1481	252.2	1.000	0.323
1582	S_1	62.3	591	48.9	.242	31.1	.0263	1484	251.8	.977	.267
1585	S_2	62.0	765	49.2	.283	40.6	.0175	1356	110.5	.972	.176
1589	S_2	61.7	759	50.5	.292	41.6	.0204	1438	164.2	.971	------
Model 10											
1357	S_1	62.1	590	49.6	0.246	31.6	0.0265	1476	165.5	1.004	------
1371	S_2	62.2	757	48.5	.276	39.5	.0220	1477	149.7	1.003	------
1381	C_2	62.7	895	49.1	.306	46.9	.0179	1476	101.5	1.001	------
1386	C_1	41.8	836	33.2	.300	44.4	.0210	1499	64.0	1.001	------
216	C_2	61.9	897	50.3	.319	48.7	.0170	1467	81	.824	0.168
223	C_1	41.4	849	34.8	.310	46.4	.0182	1462	43.4	.838	.202
229	S_2	61.7	754	50.0	.287	40.9	.0206	1464	140.5	.994	.2370
317	C_2	61.8	895	48.9	.310	47.4	.0173	1477	92.7	.958	.143
693	C_1	41.3	584	33.9	.251	32.1	.0253	1461	98.3	.962	.254
170	S_1	61.8	760	49.4	.285	40.7	.0217	1496	156.5	1.006	.293
174	C_1	41.2	840	32.1	.293	43.9	.0194	1488	53.0	1.008	.251
86	S_1	62.3	590	51.4	.255	32.6	.0249	1471	231	1.282	.329
95	S_2	65.5	759	51.0	.292	41.5	.0206	1468	151	1.214	.243
99	C_2	62.5	898	50.7	.320	48.8	.0170	1471	99.2	.979	.355
1498	C_1	41.7	843	31.9	.288	43.2	.0157	1372	639.1	.989	.235
324	S_1	62.3	587	50.6	.249	31.9	.0252	1476	222	1.014	.397
83	C_1	41.6	841	31.6	.286	42.8	.0196	1500	52.6	.985	.190
Model 10A											
530	S_1	62.3	587	49.5	0.244	31.3	0.0260	1497	229.2	0.980	0.352
572	S_2	62.5	758	49.6	.283	40.4	.0214	1481	156.8	.981	.332
598	C_2	61.9	899	49.5	.315	48.1	.0175	1464	97.1	0	.226

TEST RESULTS

Combustor performance characteristics										
Stator factor, δ_{stot}	Rotor factor, δ_{rot}	Combustor average temperature rise, K	Combustor pressure loss, percent	Combustion efficiency, η_o, percent	HC emissions index, g/kg of fuel	CO emission index, g/kg of fuel	NO_x emission index, g/kg of fuel	Combustion efficiency, η_{cc}, percent	FARR	FARRO
Model 1B										
0.329	0.082	914	5.75	102.8	-----	-----	-----	------	-----	-----
.267	.026	716	7.40	102.0	-----	-----	-----	------	-----	-----
.174	.014	634	8.14	101.3	-----	-----	-----	------	-----	-----
.175	.007	583	8.52	101.2	-----	-----	-----	------	-----	-----
Model 3										
0.554	0.103	798	5.20	103.7	0.000	3.72	5.63	99.9	0.909	0.815
.396	.100	787	5.39	104.5	-----	-----	-----	------	-----	-----
Model 6										
0.168	0.028	874	5.07	100.4	-----	-----	-----	100.5	-----	-----
.158	.009	706	6.44	99.9	-----	-----	-----	99.6	-----	-----
.145	.011	620	6.98	98.7	-----	-----	-----	98.0	-----	-----
.187	.016	886	4.88	100.8	-----	-----	-----	98.5	-----	-----
.287	.022	621	6.83	100.3	-.03	2.77	12.38	99.9	0.787	-----
.158	.014	571	7.25	100.7	.09	1.65	16.82	100.0	.728	-----
Model 7										
0.302	0.032	891	4.37	100.8	0.06	2.6	6.85	99.3	0.977	1.096
.267	.016	893	4.07	99.4	.07	5.1	5.77	99.9	1.013	1.019
.243	.036	591	5.18	99.0	.03	3.2	9.21	99.9	.966	1.036
-----	-----	---	5.51	-----	.06	2.41	9.61	99.9	.962	1.042
Model 10										
-----	-----	886	5.75	-----	0	5.0	5.6	99.9	0.952	0.986
-----	-----	720	6.77	-----	.02	1.9	9.5	99.95	.939	.942
-----	-----	581	7.93	-----	0	1.5	15.5	99.97	.973	.960
-----	-----	663	8.42	-----	0	2.4	10.2	99.9	.941	.928
0.212	0.059	570	8.55	100.3	1.1	7.7	13.6	99.7	.859	-----
.267	.056	613	8.25	100.1	.5	8.3	9.5	99.8	.841	-----
.253	.063	710	7.16m	101.7	1.85	8.4	8.5	99.6	.791	-----
.201	.087	582	8.26	101.0	.85	5.3	10.8	99.7	.727	-----
.253	.030	876	6.02	101.2	.02	14.9	5.7	99.6	1.096	-----
.292	.044	736	7.24	101.4	-----	-----	-----	------	-----	-----
.250	.074	648	7.46	100.9	-----	-----	-----	------	-----	-----
.329	.075	881	5.99	103.1	-----	-----	-----	------	-----	-----
.268	.106	709	7.51	102.5	-----	-----	-----	------	-----	-----
.307	.088	573	8.45	101.9	-----	-----	-----	------	-----	-----
.299	.123	530	7.06	99.5	.02	1.3	10.6	100.0	.962	.990
.360	.014	889	5.79	102.9	.58	7.38	3.9	99.7	.663	-----
.250	.092	659	7.36	101.2	-----	-----	-----	------	-----	-----
Model 10A										
0.316	0.055	910	5.22	102.9	0.03	8.61	5.53	99.9	1.512	-----
.286	.027	723	6.83	100.8	.02	3.16	9.27	99.9	.916	-----
.196	.020	565	7.9	97.9	.06	5.06	11.4	99.8	.807	-----

TABLE VI. - COMBUSTOR ACCUMULATED BURN TIME

Model	Time	Relative condition
1A	164.0 } 174.3 hr	Some burning of scoop lips and sides of long center scoops
1B	10.3 }	
3	5.3	No damage, very little metal oxidation
6	105.1	Some burning of scoop lips; long center scoops ballooned; and some scoop turning vanes lost
7	16.3	Same as model 6
10	127.8	Same as model 6
10A	20.4	Some burning of short center scoops

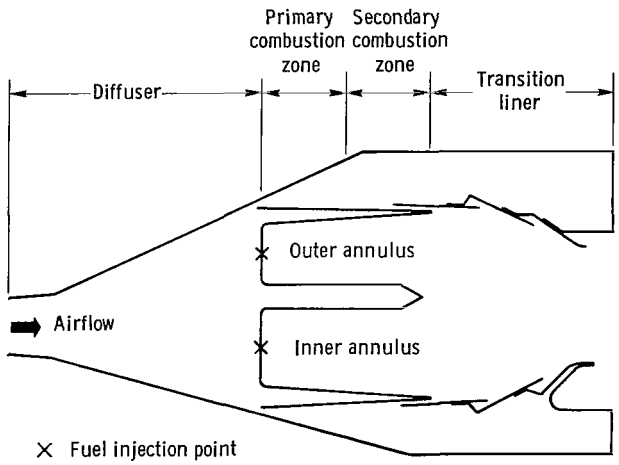

Figure 1. - Typical double-annular combustor with open diffuser.

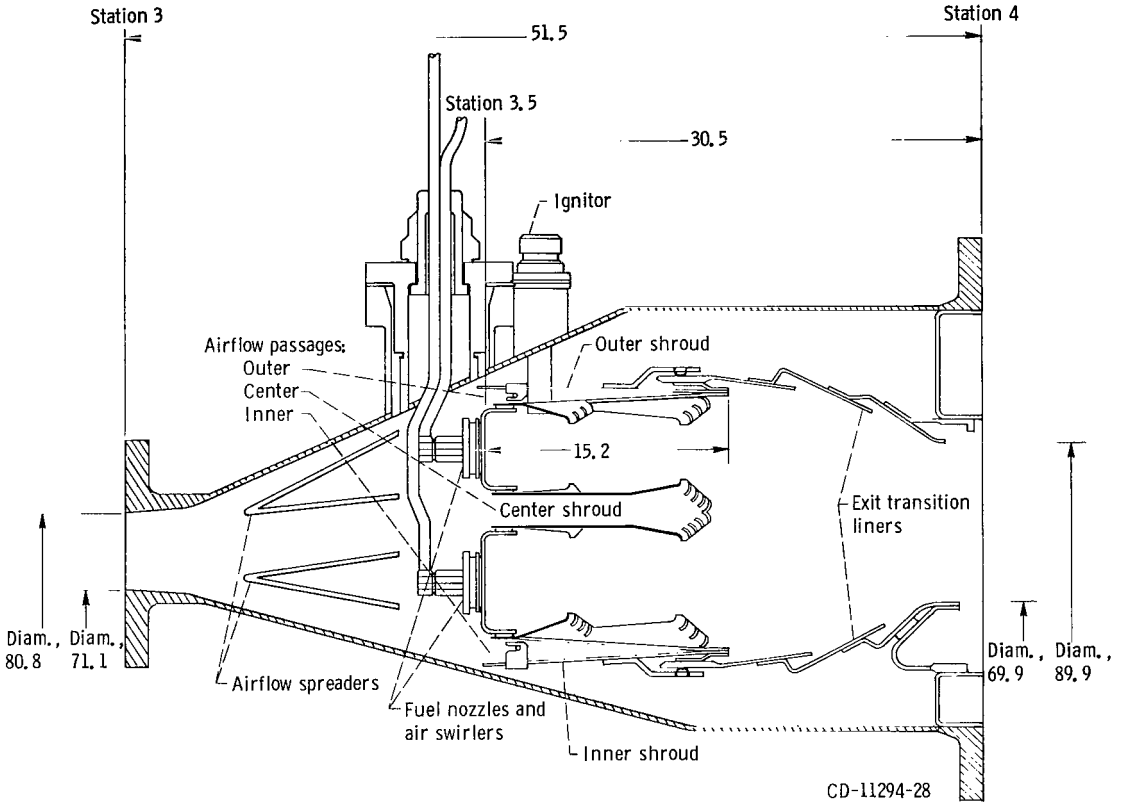

Figure 2. - Cross section of double-annular ram-induction combustor. (All dimensions are in cm.)

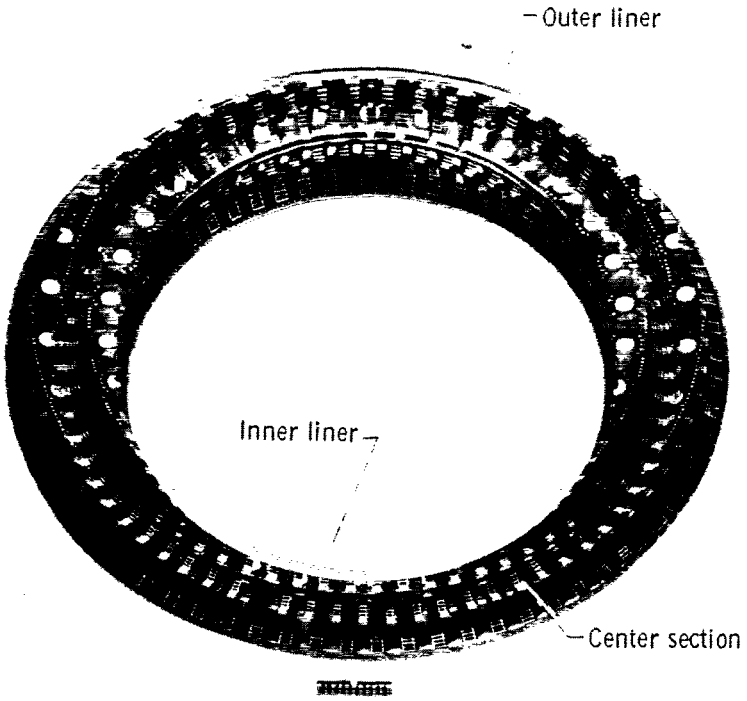

(a) Viewed from downstream (fuel nozzles removed).

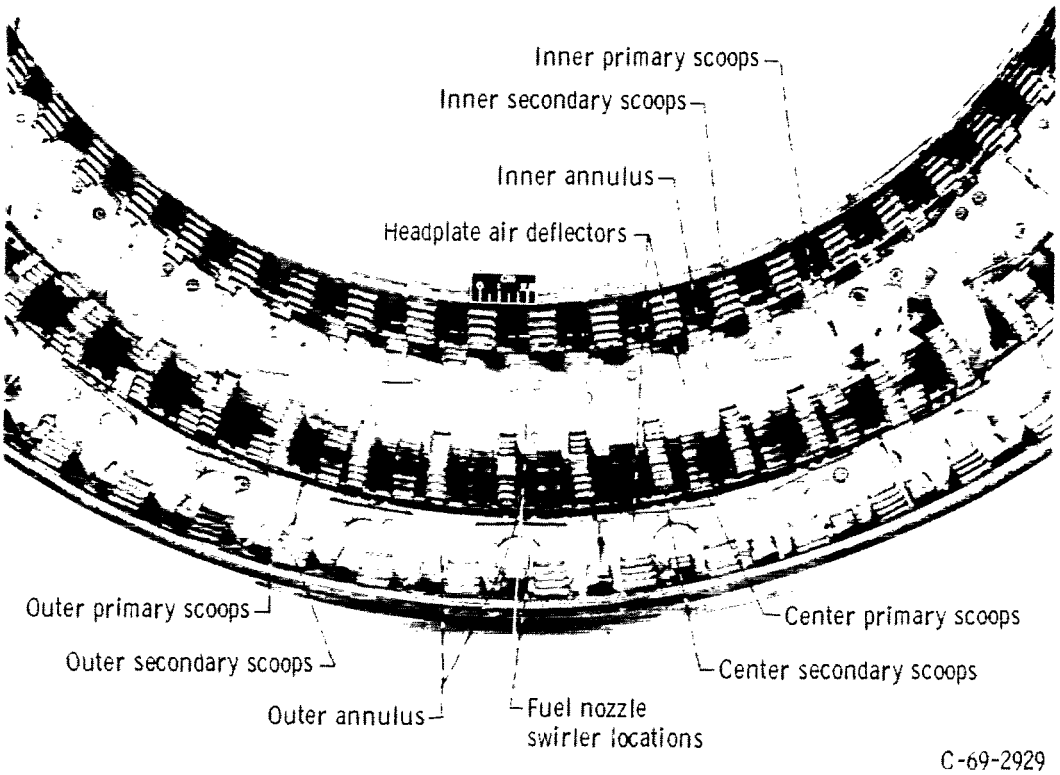

(b) Closeup view.

Figure 3. - Double-annular ram-induction combustor with 512 air scoops.

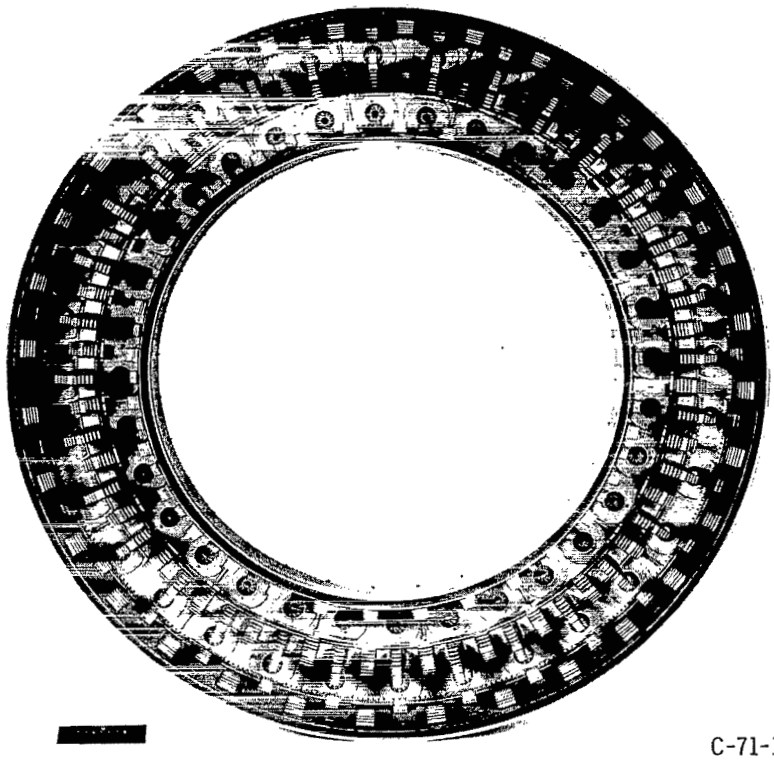

C-71-1998

(a) Viewed from downstream.

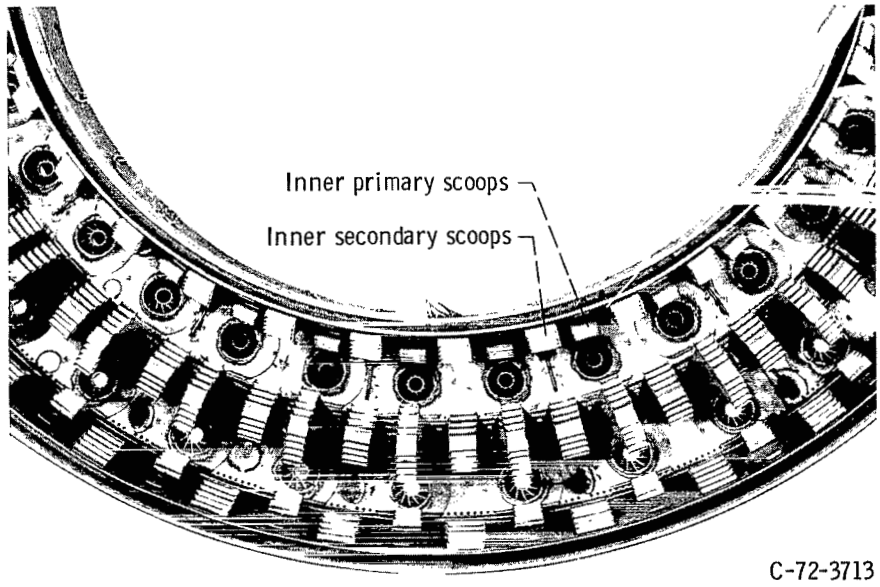

C-72-3713

(b) Closeup view.

Figure 4. - Double-annular ram-induction combustor with 256 air scoops.

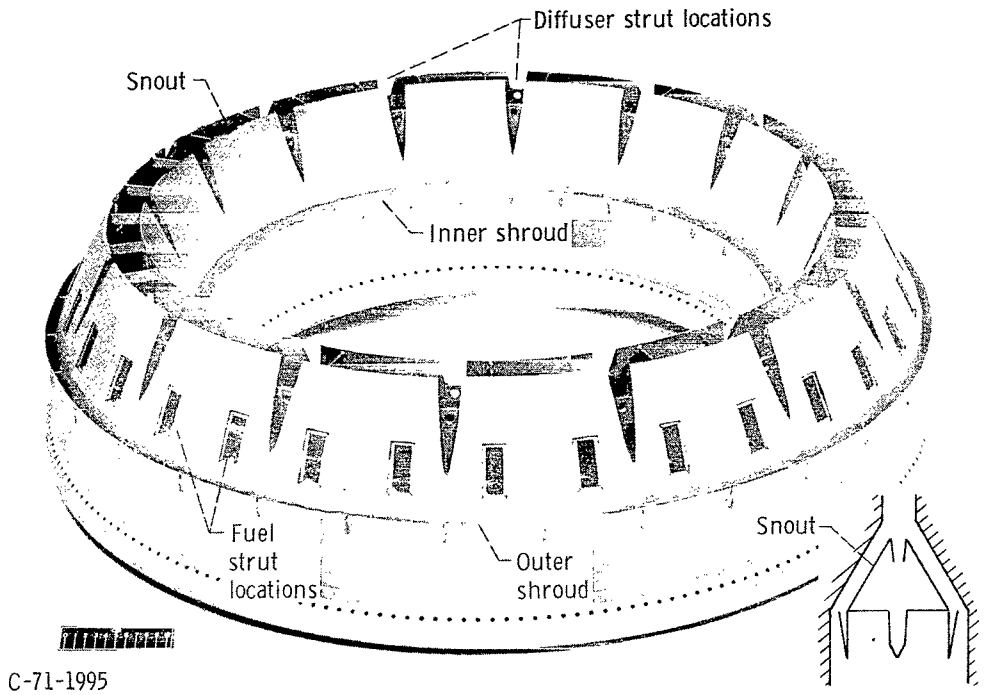

(a) Combustor with snout.

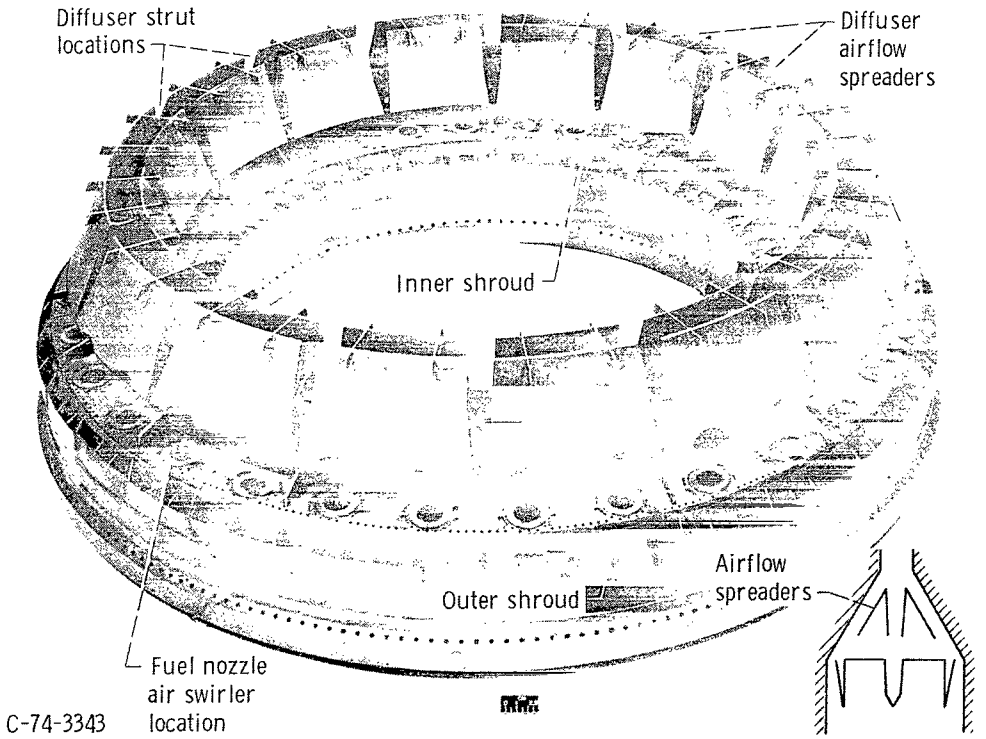

(b) Combustor with airflow spreaders.

Figure 5. - Sideviews showing combustor snouts and airflow spreaders.

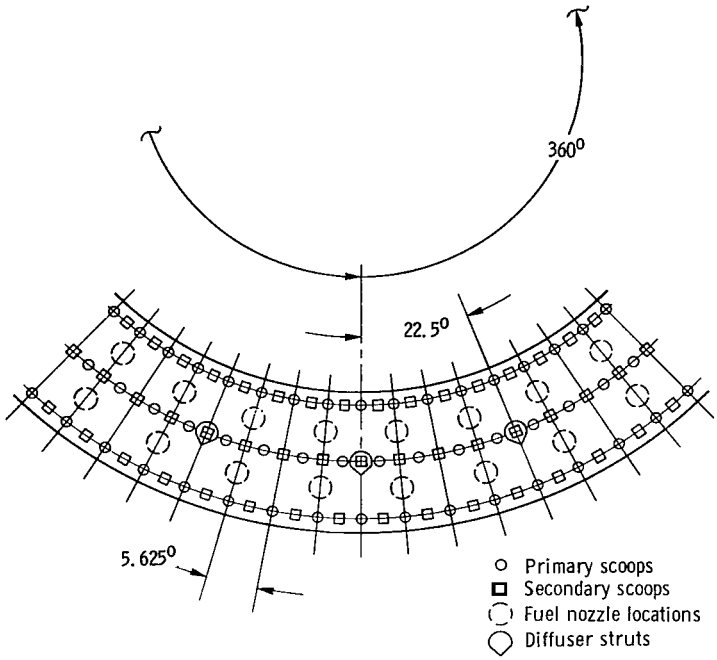

(a) Combustor with 512 scoops.

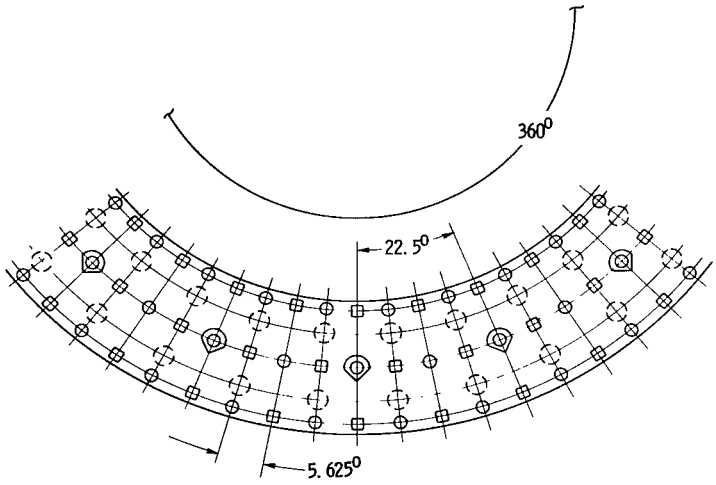

(b) Combustor with 256 scoops.

Figure 6. - Circumferential arrangement of combustor scoops and fuel nozzles.

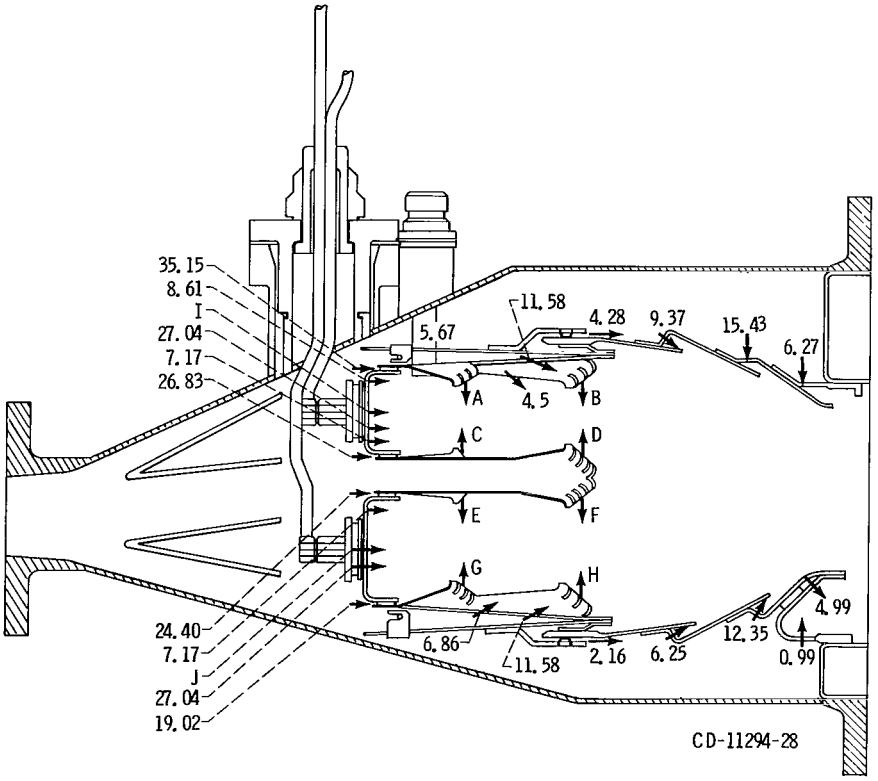

Figure 7. - Effective flow area distribution for double-annular ram-induction combustor. Swirler discharge coefficient, 0.50; hole discharge coefficient, 0.62; scoops and slot discharge coefficient, 1.00. (All areas are based on full annulus with units of cm^2.) Letter code refers to table III.

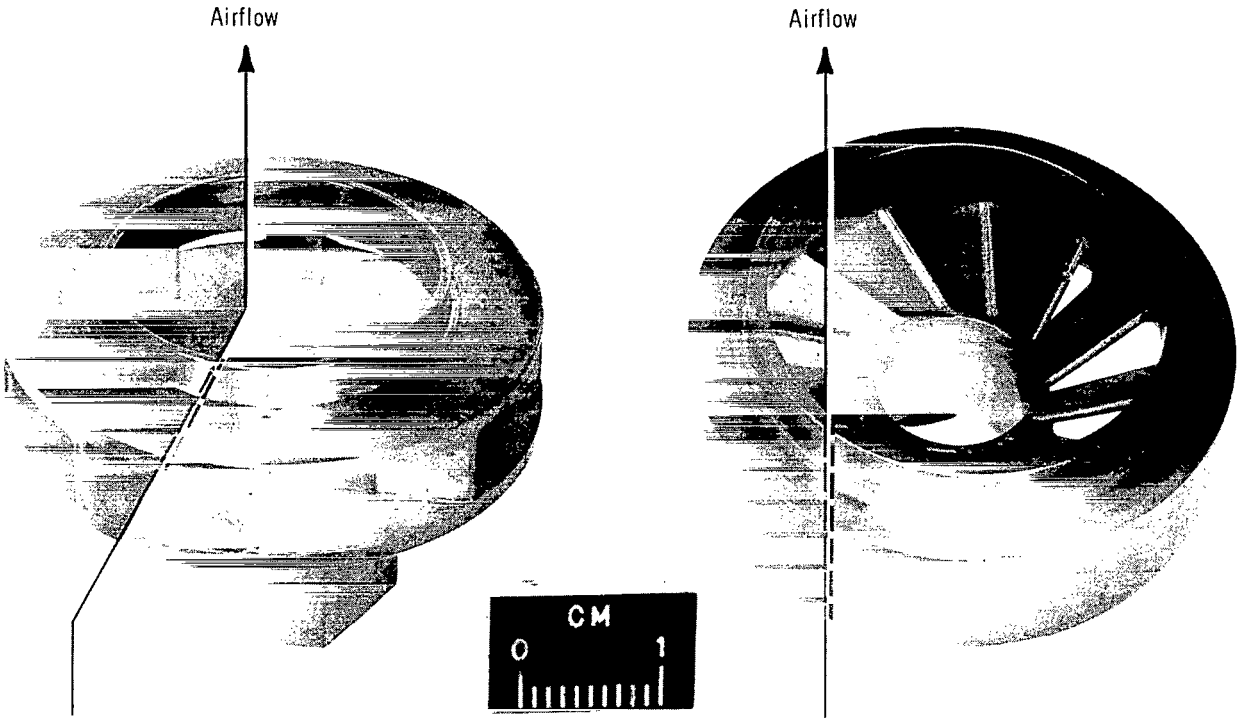

(a) Radial inflow.

(b) Axial flow.

Figure 8. - Comparison of radial inflow and axial flow air swirlers used in this study.

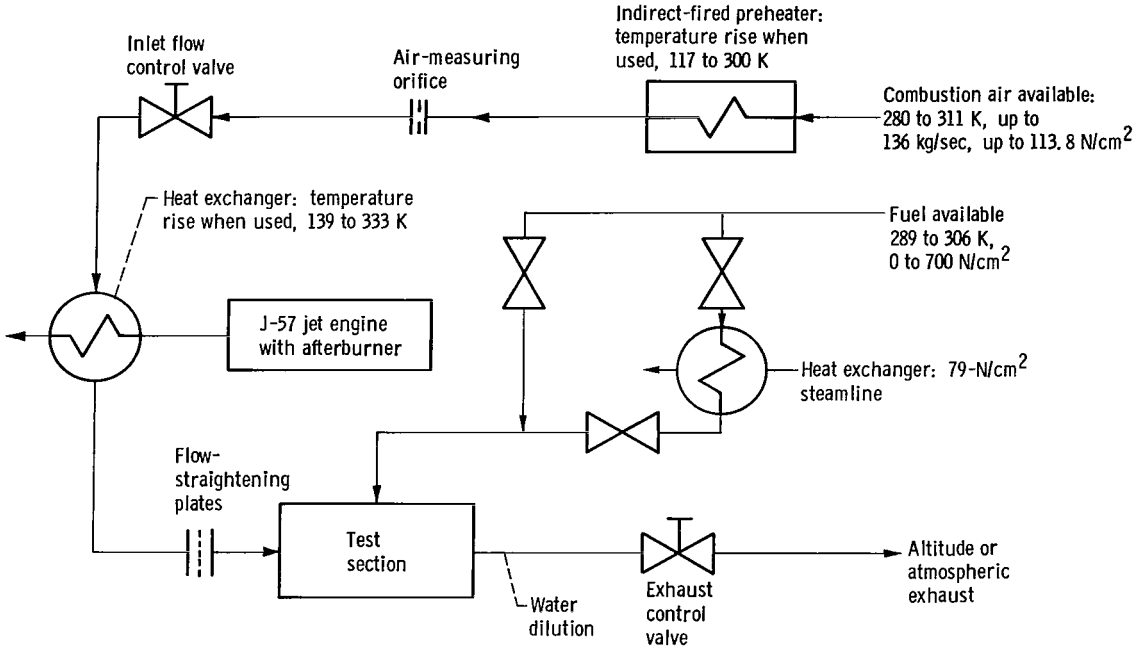

Figure 9. - Schematic of test facility combustion air and fuel.

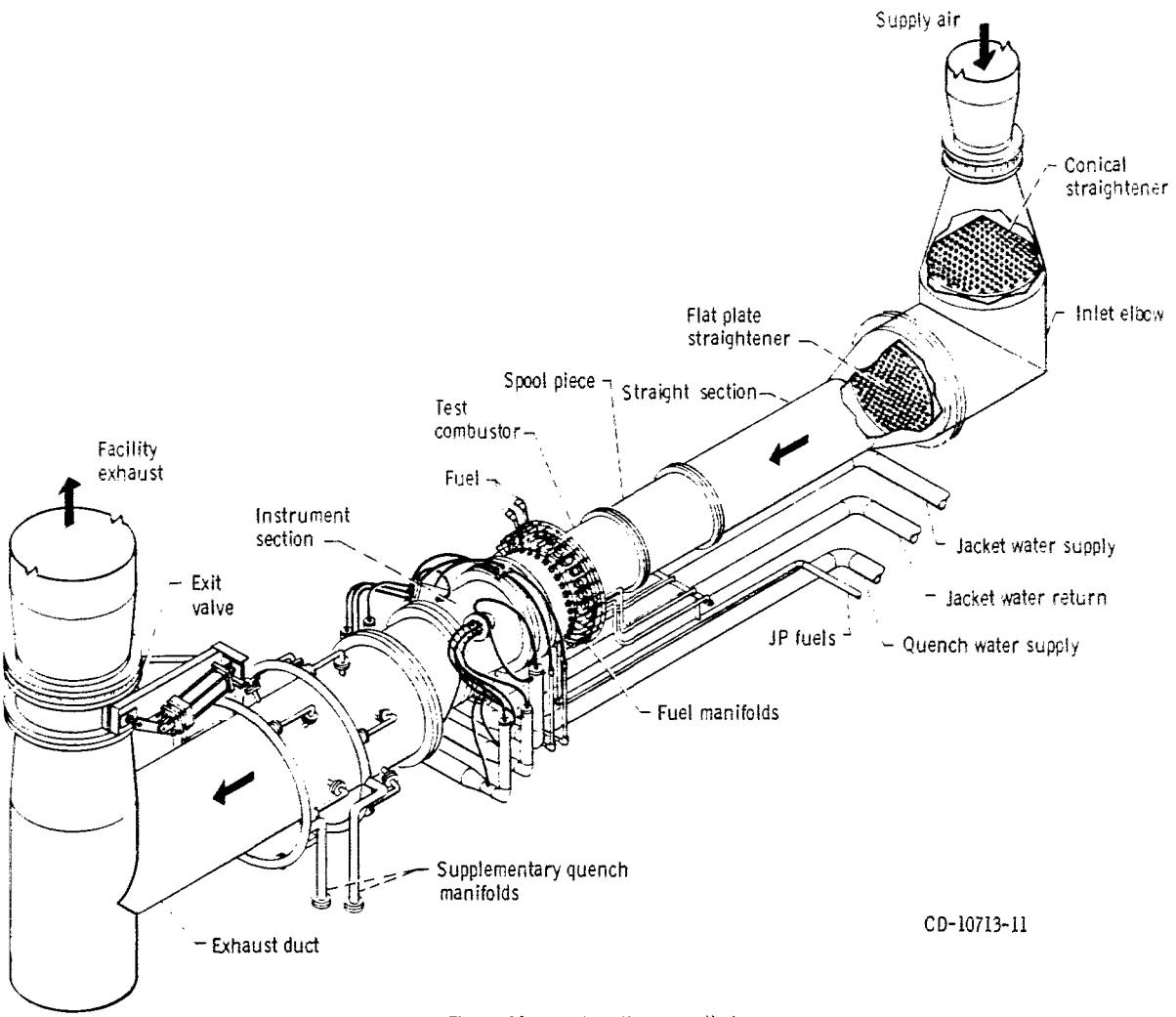

Figure 10. - Test section overall view.

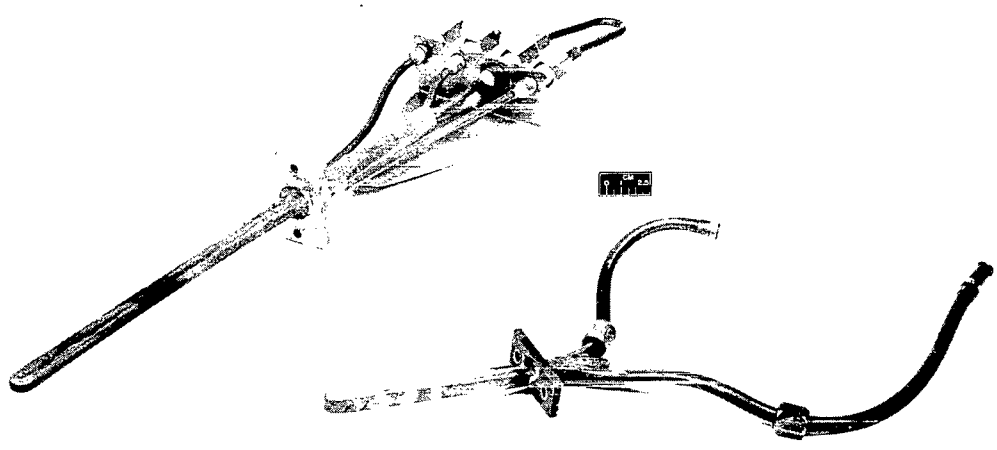

C-74-3476

(a) Fixed probe. (b) Rotating probe.

Figure 11. - Exhaust gas sample probes (water cooled).

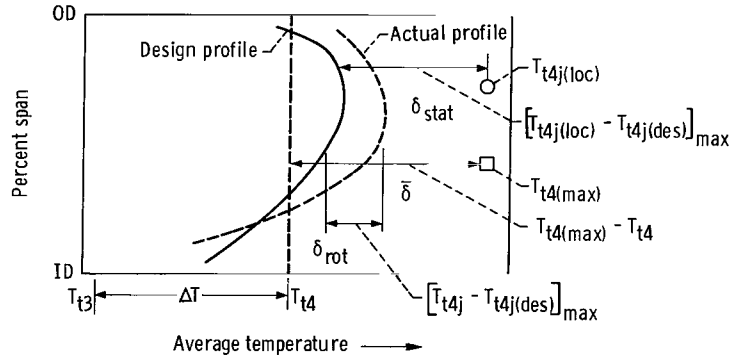

Figure 12. - Explanation of terms in exit temperature profile parameters.

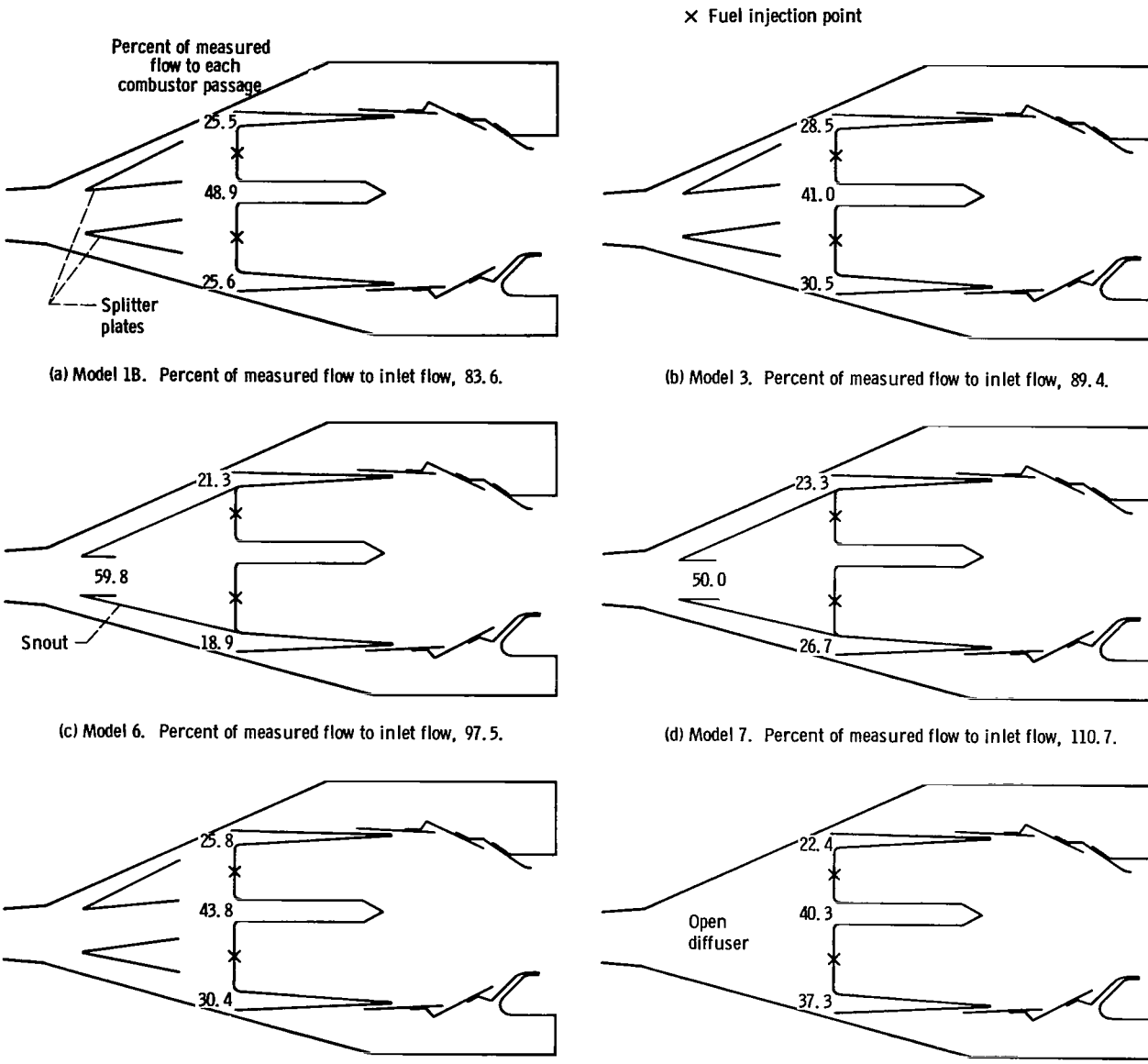

(a) Model 1B. Percent of measured flow to inlet flow, 83.6.

(b) Model 3. Percent of measured flow to inlet flow, 89.4.

(c) Model 6. Percent of measured flow to inlet flow, 97.5.

(d) Model 7. Percent of measured flow to inlet flow, 110.7.

(e) Model 10. Percent of measured flow to inlet flow, 89.2.

(f) Model 10A. Percent of measured flow to inlet flow, 90.0.

Figure 13. - Comparison of diffuser airflow distribution between combustors.

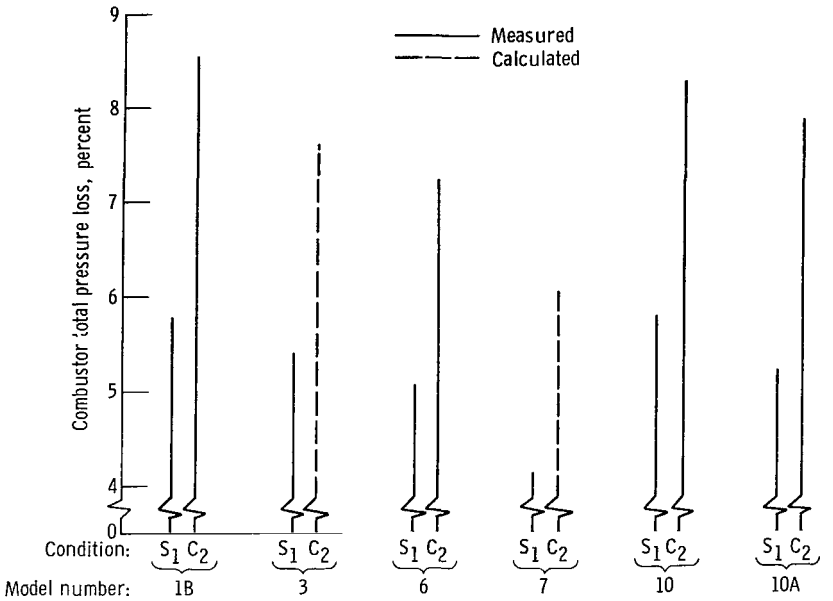

Figure 14. - Comparison of combustor total pressure loss at Mach 3.0 cruise C_2 and simulated takeoff S_1 conditions with 1478 K average exit temperature and 62-newton-per-square-centimeter inlet total pressure. S_1 indicates simulated takeoff at combustor inlet air temperature T_3 = 585 K, pressure ratio PR ≅ 12 to 1, and reference velocity V_{ref} = 30.5 meters per second; C_2 indicates Mach 3.0 cruise at combustor inlet air temperature T_3 = 895 K and reference velocity V_{ref} = 45 meters per second.

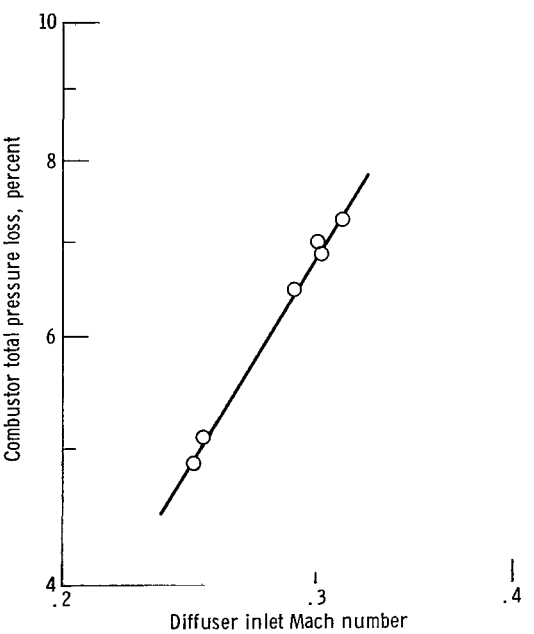

Figure 15. - Combustor total pressure loss including diffuser loss as a function of diffuser inlet Mach number for model 6 combustor.

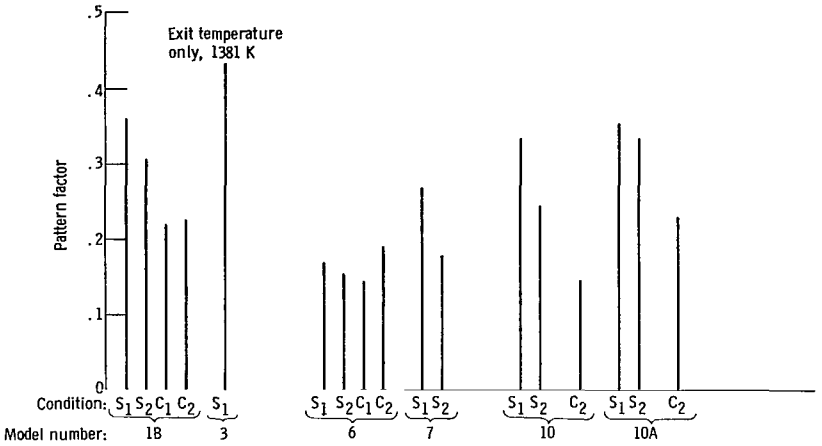

(a) Pattern factor.

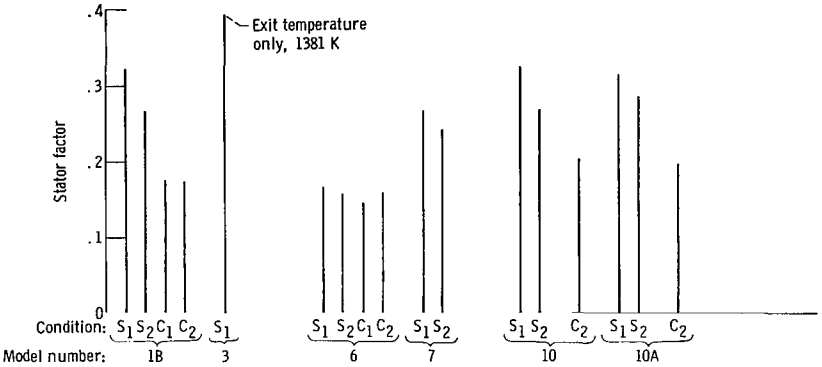

(b) Stator factor.

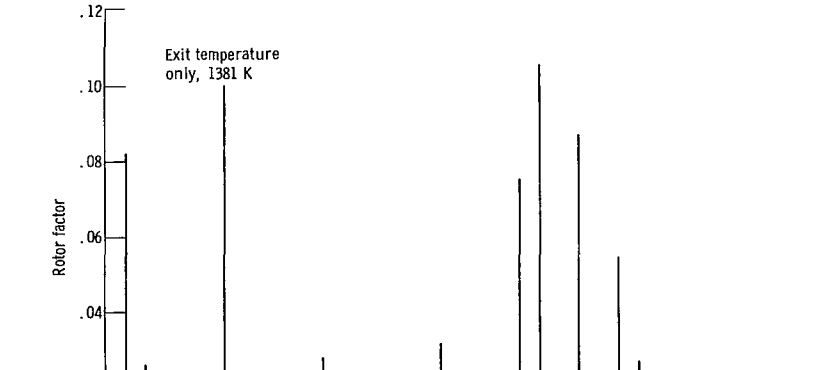

(c) Rotor factor.

Figure 16. - Comparison of exit temperature profile parameters for combustor models tested at exit average temperature of 1478 K. S_1 indicates simulated takeoff at combustor inlet air temperature T_3 = 585 K, pressure ratio PR ≅ 12 to 1, and reference velocity V_{ref} = 30.5 meters per second; S_2 indicates simulated takeoff at combustor inlet air temperature T_3 = 755 K, pressure ratio PR ≅ 23 to 1, and reference velocity V_{ref} = 41.3 meters per second; C_1 indicates Mach 2.7 cruise at combustor inlet air temperature T_3 = 840 K and reference velocity V_{ref} = 44.7 meters per second; C_2 indicates Mach 3.0 cruise at combustor inlet air temperature T_3 = 895 K and reference velocity V_{ref} = 45 meters per second.

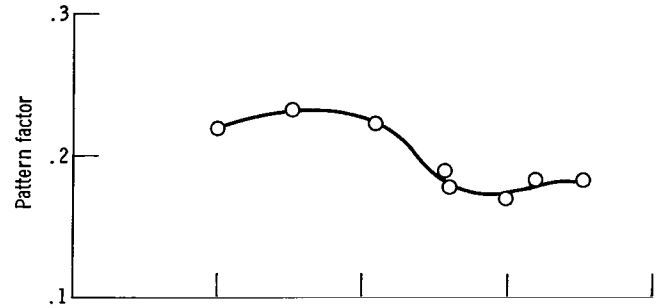

(a) Pattern factor.

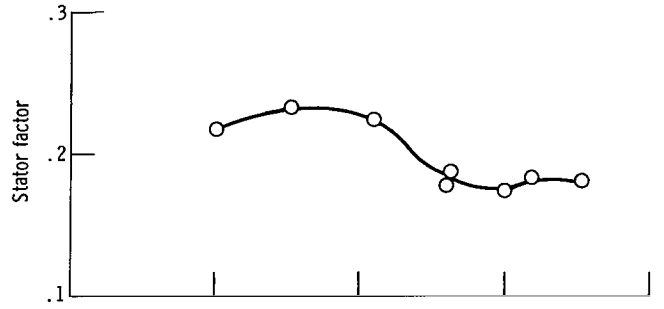

(b) Stator factor.

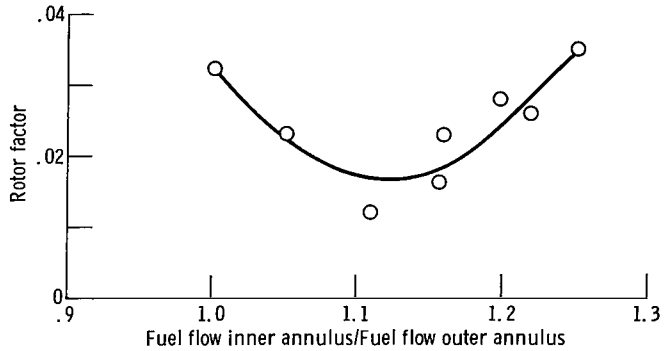

(c) Rotor factor.

Figure 17. - Effect of radial fuel staging on combustor exit temperature profile parameters of pattern factor, rotor factor, and stator factor using model 6 combustor at simulated takeoff condition. Inlet total pressure, 62 newtons per square centimeter; inlet temperature, 590 K; reference velocity, 32 meters per second; exit average temperature, 1475 K.

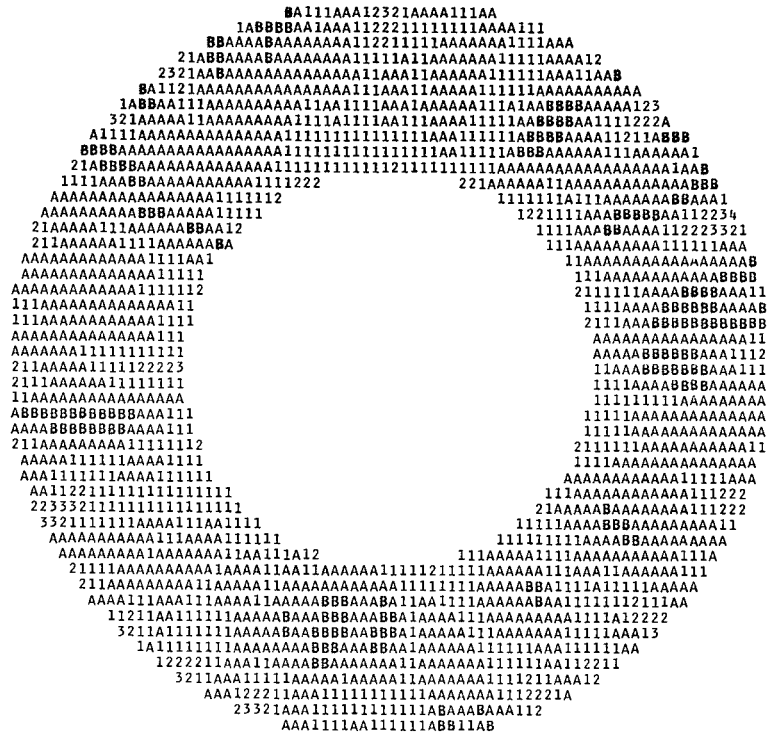

Local factor	range
J	1.00 to 0.90
I	.90 to .80
H	.80 to .70
G	.70 to .60
F	.60 to .50
E	.50 to .40
D	.40 to .30
C	.30 to .20
B	.20 to .10
A	.10 to .00
1	.00 to -.10
2	-.10 to -.20
3	-.20 to -.30
4	-.30 to -.40
5	-.40 to -.50
6	-.50 to -.60
7	-.60 to -.70
8	-.70 to -.80
9	-.80 to -.90
0	-.90 to -1.00

(a) Model 6 at condition S_1 (simulated takeoff at combustor inlet air temperature T_3 = 585 K, pressure ratio PR ≅ 12 to 1, and reference velocity V_{ref} = 30.5 m/sec). Inlet total pressure, 62 newtons per square centimeter; inlet temperature, 590 K; exit average temperature, 1478 K; pattern factor, 0.169.

Figure 18. - Circumferential exit temperature expressed in terms of local factor.

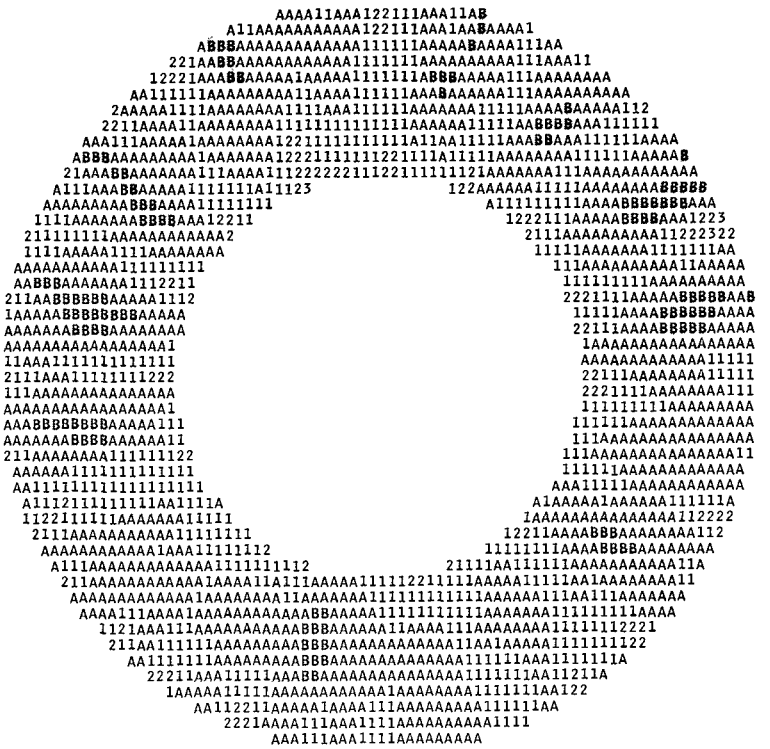

	Local factor range
J	1.00 to 0.90
I	.90 to .80
H	.80 to .70
G	.70 to .60
F	.60 to .50
E	.50 to .40
D	.40 to .30
C	.30 to .20
B	.20 to ,10
A	.10 to .00
1	.00 to -.10
2	-.10 to -.20
3	-.20 to -.30
4	-.30 to -.40
5	-.40 to -.50
6	-.50 to -.60
7	-.60 to -.70
8	-.70 to -.80
9	-.80 to -.90
0	-.90 to -1.00

(b) Model 6 at condition S_2 (simulated takeoff at combustor inlet air temperature T_3 = 755 K, pressure ratio PR ≅ 23 to 1, and reference velocity V_{ref} = 41.3 m/sec). Inlet total pressure, 62 newtons per square centimeter; inlet temperature, 755 K; reference velocity, 40.7 meters per second; exit average temperature, 1478 K; pattern factor, 0.154.

Figure 18. - Continued.

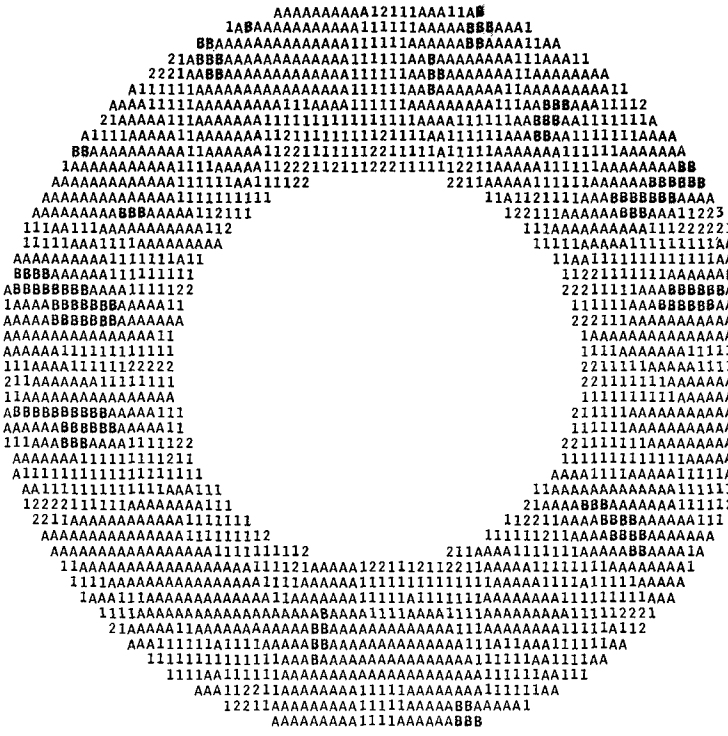

	Local factor range
J	1.00 to 0.90
I	.90 to .80
H	.80 to .70
G	.70 to .60
F	.60 to .50
E	.50 to .40
D	.40 to .30
C	.30 to .20
B	.20 to .10
A	.10 to .00
1	.00 to -.10
2	-.10 to -.20
3	-.20 to -.30
4	-.30 to -.40
5	-.40 to -.50
6	-.50 to -.60
7	-.60 to -.70
8	-.70 to -.80
9	-.80 to -.90
0	-.90 to -1.00

(c) Model 6 at condition C_1 (Mach 2.7 cruise at combustor inlet air temperature T_3 = 840 K and reference velocity V_{ref} = 44.7 m/sec). Inlet total pressure, 41 newtons per square centimeter; reference velocity, 42.7 meters per per second; exit average temperature, 1478 K; pattern factor, 0.145.

Figure 18. - Continued.

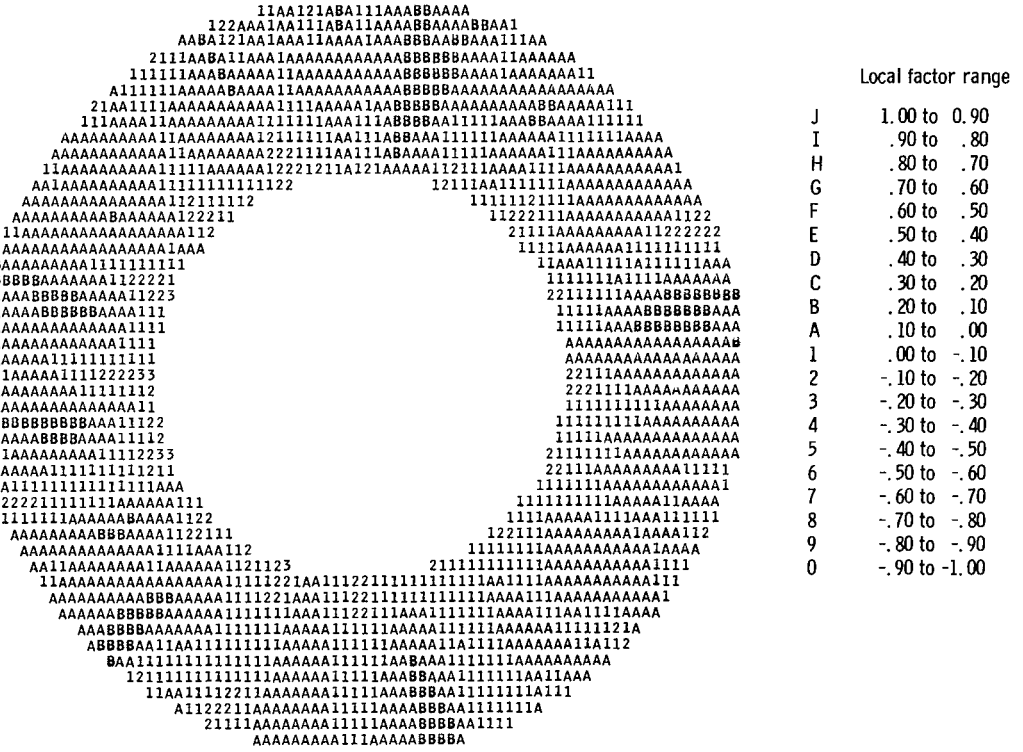

(d) Model 6 at condition C_2 (Mach 3.0 cruise at combustor inlet air temperature T_3 = 840 K and reference velocity V_{ref} = 45 m/sec). Inlet total pressure, 62 newtons per square centimeter; inlet temperature, 895 K; reference velocity, 45.7 meters per second; exit average temperature, 1478 K; pattern factor, 0.187.

Figure 18. - Continued.

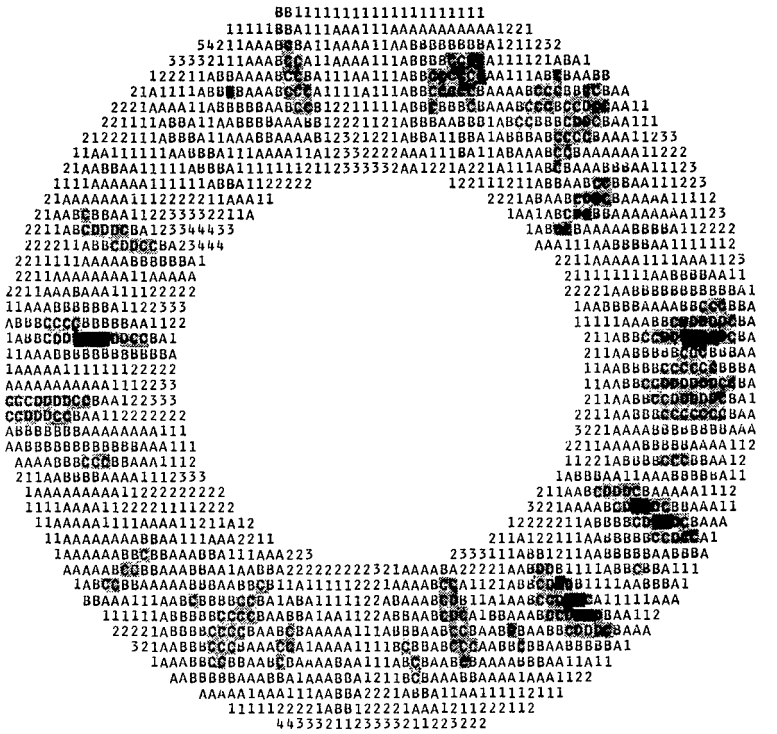

Local factor range	
J	1.00 to 0.90
I	.90 to .80
H	.80 to .70
G	.70 to .60
F	.60 to .50
E	.50 to .40
D	.40 to .30
C	.30 to .20
B	.20 to .10
A	.10 to .00
1	.00 to -.10
2	-.10 to -.20
3	-.20 to -.30
4	-.30 to -.40
5	-.40 to -.50
6	-.50 to -.60
7	-.60 to -.70
8	-.70 to -.80
9	-.80 to -.90
0	-.90 to -1.00

(e) Model 3 at condition S_1 (simulated takeoff at combustor inlet air temperature T_3 = 585 K; pressure ratio PR ≅ 23 to 1, and reference velocity V_{ref} = 30.5 m/sec). Inlet total pressure, 62 newtons per square centimeter; inlet temperature, 590 K; exit average temperature reduced to 1389 K; pattern factor, 0.588.

Figure 18. - Concluded.

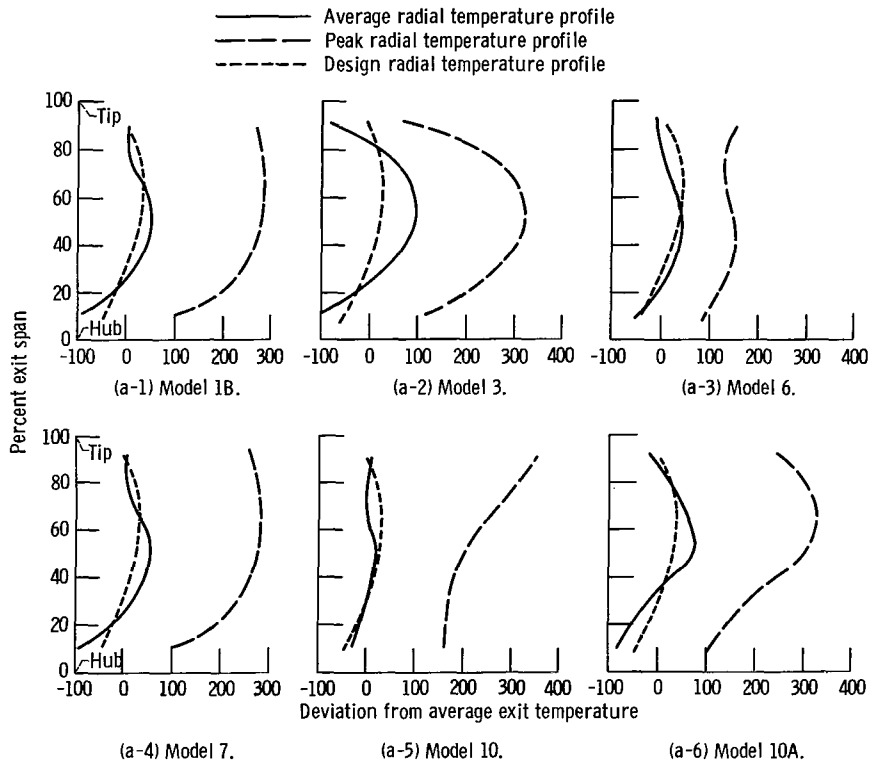

(a) Simulated takeoff condition of 62-newton-per-square-centimeter inlet total pressure, 589 K inlet temperature, and 30.5-meter-per-second reference velocity.

Figure 19. - Comparison of radial average and peak temperature profiles for combustor models tested at an exit temperature of 1478 K except model 3 which was tested at 1367 K.

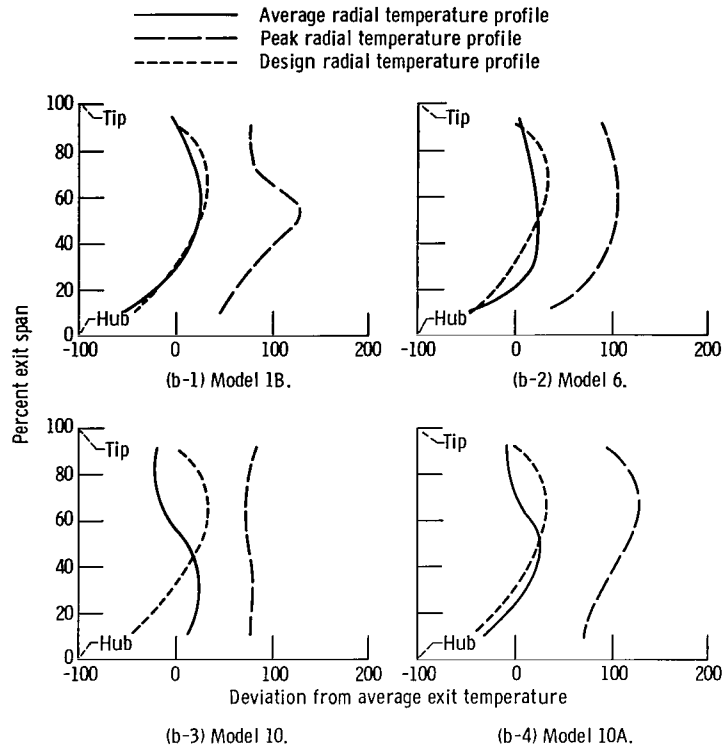

(b) Simulated Mach 3.0 cruise condition of 62-newton-per-square-centimeter inlet total pressure, 895 K inlet temperature, and 48-meter-per-second reference velocity.

Figure 19. - Concluded.

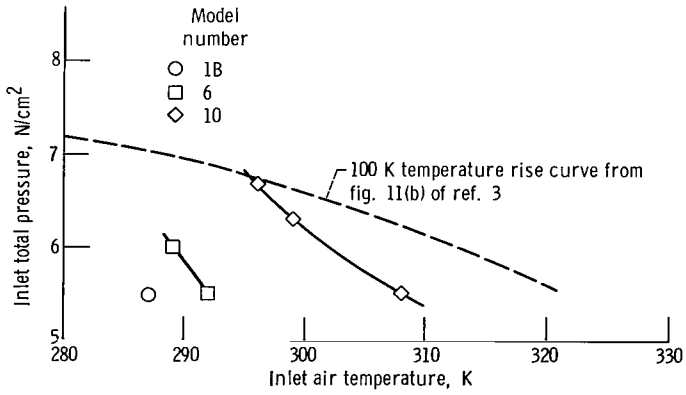

Figure 20. - Minimum inlet pressure for which ignition with 80 K temperature rise could be obtained with combustor reference Mach number of 0.05.

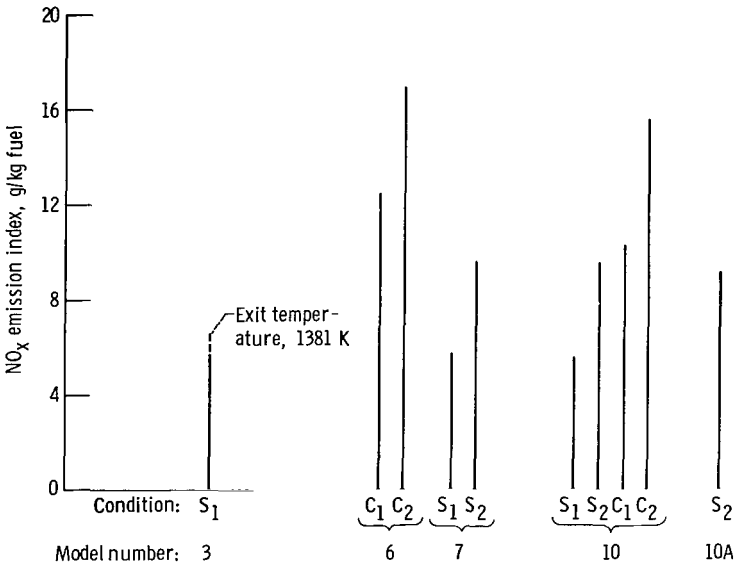

Figure 21. - Comparison of NO_x emissions index for combustor models tested at exit average temperature of 1478 K. S_1 indicates simulated takeoff at combustor inlet air temperature T_3 = 585 K, pressure ratio PR ≅ 12 to 1, and reference velocity V_{ref} = 30.5 meters per second; S_2 indicates simulated takeoff at combustor inlet air temperature T_3 = 755 K, pressure ratio PR ≅ 23 to 1, and reference velocity V_{ref} = 41.3 meters per second; C_1 indicates Mach 2.7 cruise at combustor inlet air temperature T_3 = 840 K and reference velocity V_{ref} = 44.7 meters per second; C_2 indicates Mach 3.0 cruise at combustor inlet air temperature T_3 = 895 K and reference velocity V_{ref} = 45 meters per second.

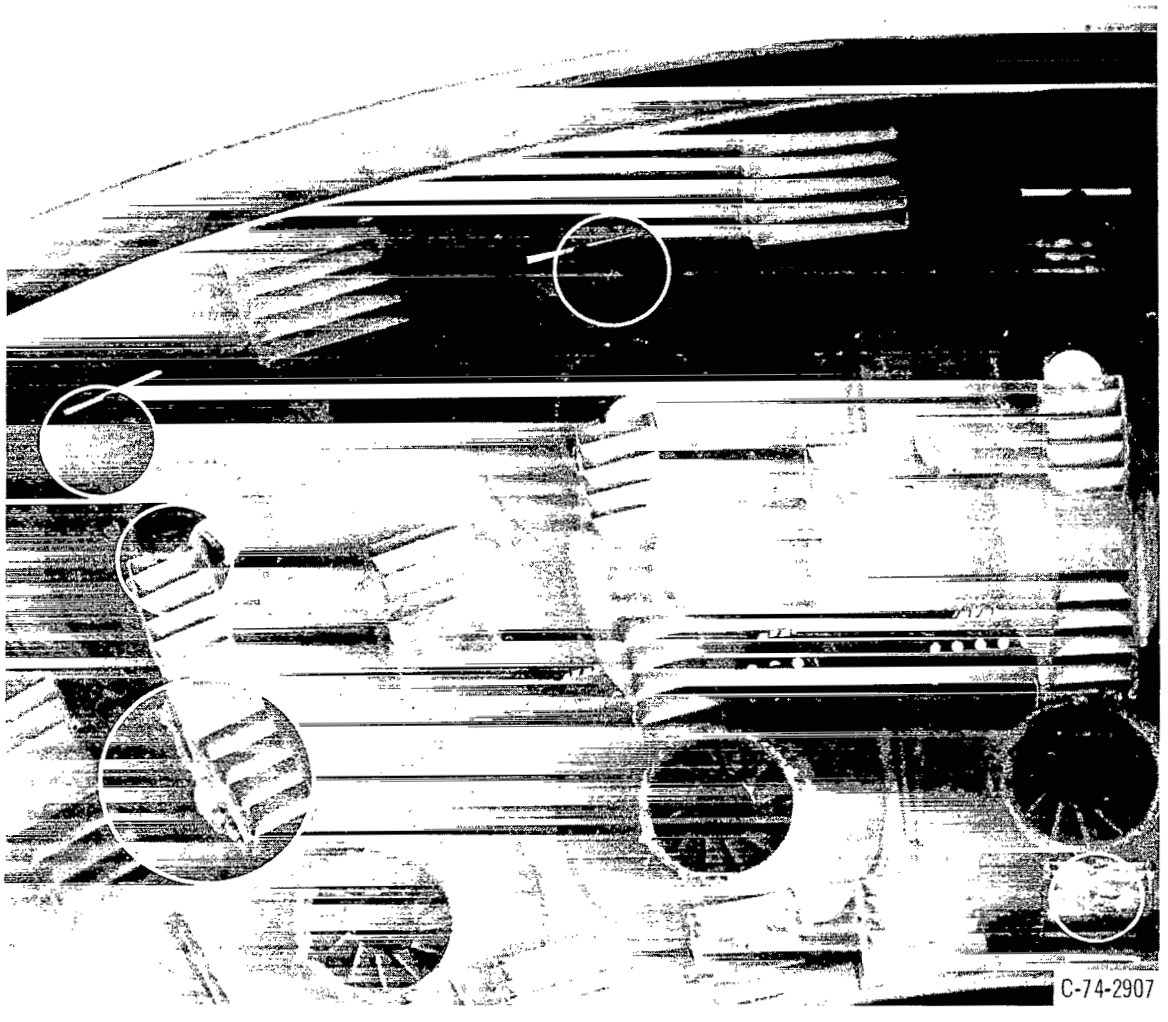

Figure 22. - Typical distress encountered by combustor models 1, 6, and 10 after over 100 hours of testing (circled areas).

NATIONAL AERONAUTICS AND SPACE ADMINISTRATION
WASHINGTON, D.C. 20546

OFFICIAL BUSINESS
PENALTY FOR PRIVATE USE $300

SPECIAL FOURTH-CLASS RATE BOOK

POSTAGE AND FEES PAID
NATIONAL AERONAUTICS AND SPACE ADMINISTRATION
451

U.S.MAIL

"The aeronautical and space activities of the United States shall be conducted so as to contribute . . . to the expansion of human knowledge of phenomena in the atmosphere and space. The Administration shall provide for the widest practicable and appropriate dissemination of information concerning its activities and the results thereof."

—NATIONAL AERONAUTICS AND SPACE ACT OF 1958

NASA SCIENTIFIC AND TECHNICAL PUBLICATIONS

TECHNICAL REPORTS: Scientific and technical information considered important, complete, and a lasting contribution to existing knowledge.

TECHNICAL NOTES: Information less broad in scope but nevertheless of importance as a contribution to existing knowledge.

TECHNICAL MEMORANDUMS: Information receiving limited distribution because of preliminary data, security classification, or other reasons. Also includes conference proceedings with either limited or unlimited distribution.

CONTRACTOR REPORTS: Scientific and technical information generated under a NASA contract or grant and considered an important contribution to existing knowledge.

TECHNICAL TRANSLATIONS: Information published in a foreign language considered to merit NASA distribution in English.

SPECIAL PUBLICATIONS: Information derived from or of value to NASA activities. Publications include final reports of major projects, monographs, data compilations, handbooks, sourcebooks, and special bibliographies.

TECHNOLOGY UTILIZATION PUBLICATIONS: Information on technology used by NASA that may be of particular interest in commercial and other non-aerospace applications. Publications include Tech Briefs, Technology Utilization Reports and Technology Surveys.

Details on the availability of these publications may be obtained from:

SCIENTIFIC AND TECHNICAL INFORMATION OFFICE

NATIONAL AERONAUTICS AND SPACE ADMINISTRATION

Washington, D.C. 20546